

Supplemental Material for "Quantum Point Contact with Local Two-Particle Loss"

Kensuke Kakimoto and Shun Uchino

CONTENTS

I. Hamiltonian formalism with noise fields	1
II. Derivation of Lindblad master equation	2
III. Keldysh formalism	4
IV. Frequency tuning	5
V. Analysis of dephasing model	7
VI. Two-particle loss: single-site case	12
VII. Two-particle loss: multi-site case	16
References	20

I. HAMILTONIAN FORMALISM WITH NOISE FIELDS

In this section, we review the Hamiltonian formalism with noise fields analogous to "white noise" in stochastic processes. In this formalism, we start with the Hamiltonian of a system coupled to an environment ($\hbar = 1$)

$$\hat{H}_{\text{tot}} = \hat{H} + \hat{H}_B + \hat{V}_\eta, \quad (\text{S1})$$

Here, \hat{H} is the system Hamiltonian and \hat{H}_B is the Hamiltonian for a heat bath defined by

$$\hat{H}_B = \int_{-\infty}^{\infty} d\omega \omega \hat{\eta}^\dagger(\omega) \hat{\eta}(\omega), \quad (\text{S2})$$

with the commutation relations

$$[\hat{\eta}(\omega), \hat{\eta}^\dagger(\omega')] = \delta(\omega - \omega'), \quad [\hat{\eta}(\omega), \hat{\eta}(\omega')] = [\hat{\eta}^\dagger(\omega), \hat{\eta}^\dagger(\omega')] = 0. \quad (\text{S3})$$

The energy spectrum of the heat bath is assumed to be continuous. The coupling between the system and the heat bath is given by

$$\hat{V}_\eta = \int_{-\infty}^{\infty} d\omega \left[\gamma(\omega) \hat{L}^\dagger \hat{\eta}(\omega) + \gamma^*(\omega) \hat{\eta}^\dagger(\omega) \hat{L} \right], \quad (\text{S4})$$

where \hat{L} is the Lindblad operator and $\gamma(\omega)$ is a coupling between the system and bath, which in general depends on frequencies.

We now consider the interaction picture under the unperturbed Hamiltonian $\hat{H} + \hat{H}_B$. In this interaction picture, the Lindblad operator is $\hat{L}(\tau) = e^{i(\hat{H} + \hat{H}_B)\tau} \hat{L} e^{-i(\hat{H} + \hat{H}_B)\tau}$, and the noise field is obtained by using the Baker-Campbell-Hausdorff formula

$$\hat{\eta}(\omega, \tau) = e^{i(\hat{H} + \hat{H}_B)\tau} \hat{\eta}(\omega) e^{-i(\hat{H} + \hat{H}_B)\tau} = e^{i\hat{H}_B\tau} \hat{\eta}(\omega) e^{-i\hat{H}_B\tau} = \hat{\eta}(\omega) e^{-i\omega\tau}. \quad (\text{S5})$$

Then, the coupling term is expressed as

$$\hat{V}_\eta(\tau) = \hat{L}^\dagger(\tau) \hat{\eta}(\tau) + \hat{\eta}^\dagger(\tau) \hat{L}(\tau), \quad (\text{S6})$$

where

$$\hat{\eta}(\tau) = \int_{-\infty}^{\infty} d\omega \gamma(\omega) \hat{\eta}(\omega) e^{-i\omega\tau}. \quad (\text{S7})$$

The operators $\hat{\eta}(t)$ obeys the following commutation relations

$$[\hat{\eta}(\tau), \hat{\eta}^\dagger(\tau')] = \int_{-\infty}^{\infty} d\omega |\gamma(\omega)|^2 e^{-i\omega(\tau-\tau')}, \quad (\text{S8})$$

and

$$[\hat{\eta}(\tau), \hat{\eta}(\tau')] = [\hat{\eta}^\dagger(\tau), \hat{\eta}^\dagger(\tau')] = 0. \quad (\text{S9})$$

Equation (S8) indicates that the commutator depends on the past history $\tau' (\neq \tau)$, resulting in non-Markovian dynamics of the system.

We next take the Markovian limit that neglects the memories of the heat bath. This corresponds to taking the frequency-independent coupling,

$$\gamma(\omega) = \sqrt{\frac{\gamma}{2\pi}}. \quad (\text{S10})$$

In this limit, the noise fields $\hat{\eta}(\omega)$ and the Lindblad operator \hat{L} are coupled with equal weight over the entire energy spectra, and it follows that

$$[\hat{\eta}(\tau), \hat{\eta}^\dagger(\tau')] = \gamma \delta(\tau - \tau'), \quad [\hat{\eta}(\tau), \hat{\eta}(\tau')] = [\hat{\eta}^\dagger(\tau), \hat{\eta}^\dagger(\tau')] = 0, \quad (\text{S11})$$

where

$$\hat{\eta}(\tau) = \sqrt{\gamma} \int_{-\infty}^{\infty} \frac{d\omega}{\sqrt{2\pi}} \hat{\eta}(\omega) e^{-i\omega\tau}. \quad (\text{S12})$$

In addition to the commutation relation, the noise field formalism considers statistical averages on noise fields. In the case of two-body loss concerned in the main text, we consider the following averages:

$$\langle \hat{\eta}(\tau) \hat{\eta}^\dagger(\tau') \rangle_\eta = \gamma \delta(\tau - \tau'), \quad \langle \hat{\eta}^\dagger(\tau) \hat{\eta}(\tau') \rangle_\eta = \langle \hat{\eta}(\tau) \hat{\eta}(\tau') \rangle_\eta = \langle \hat{\eta}^\dagger(\tau) \hat{\eta}^\dagger(\tau') \rangle_\eta = \langle \hat{\eta}(\tau) \rangle_\eta = \langle \hat{\eta}^\dagger(\tau) \rangle_\eta = 0. \quad (\text{S13})$$

The above averages of the noise fields correspond to the assumption that the heat bath is in the vacuum state $\langle \cdots \rangle_\eta = \langle \text{vac} | \cdots | \text{vac} \rangle$ with $\hat{\eta}(\tau) | \text{vac} \rangle = 0$. Physically, this indicates that the population of particles outside the system is absent and therefore no particle injection from outside.

II. DERIVATION OF LINDBLAD MASTER EQUATION

In this section, we derive the Lindblad master equation using the noise fields. The density operator of the total system obeys the von Neumann equation in the Schrödinger picture

$$\frac{\partial}{\partial \tau} \hat{\rho}_{\text{tot}}(\tau) = -i [\hat{H}_{\text{tot}}, \hat{\rho}_{\text{tot}}(\tau)]. \quad (\text{S14})$$

By dividing the Hamiltonian into an unperturbed part $\hat{H} + \hat{H}_B$ and a perturbed part \hat{V}_η , we construct the interaction picture

$$\frac{\partial}{\partial \tau} \hat{\rho}_{\text{tot}, I}(\tau) = -i [\hat{V}_\eta(\tau), \hat{\rho}_{\text{tot}, I}(\tau)], \quad (\text{S15})$$

where $\hat{\rho}_{\text{tot}, I}(\tau) = e^{i(\hat{H} + \hat{H}_B)\tau} \hat{\rho}_{\text{tot}}(\tau) e^{-i(\hat{H} + \hat{H}_B)\tau}$ and $\hat{V}_\eta(\tau)$ is defined as Eq. (S6). Here, the subscript I denotes the interaction picture. By formally solving Eq. (S15)

$$\hat{\rho}_{\text{tot}, I}(\tau) = \hat{\rho}_{\text{tot}, I}(0) - i \int_0^\tau d\tau' [\hat{V}_\eta(\tau'), \hat{\rho}_{\text{tot}, I}(\tau')], \quad (\text{S16})$$

Eq. (S15) can be rewritten

$$\frac{\partial}{\partial \tau} \hat{\rho}_{\text{tot},I}(\tau) = -i \left[\hat{V}_\eta(\tau), \hat{\rho}_{\text{tot},I}(0) \right] - \int_0^\tau d\tau' \left[\hat{V}_\eta(\tau), \left[\hat{V}_\eta(\tau'), \hat{\rho}_{\text{tot},I}(\tau') \right] \right]. \quad (\text{S17})$$

The density operator of the system is defined as

$$\hat{\rho}_I(\tau) = \text{Tr}_B \{ \hat{\rho}_{\text{tot},I}(\tau) \}. \quad (\text{S18})$$

The partial trace over the environment is associated with the noise average as follows:

$$\langle \cdots \rangle_\eta = \text{Tr}_B \{ \hat{\rho}_B(0) (\cdots) \}. \quad (\text{S19})$$

Here, $\hat{\rho}_B$ is the density operator of the heat bath. To obtain an equation of motion for $\hat{\rho}_I(\tau)$, we consider the following conditions [1]:

1. Initial state: $\hat{\rho}_{\text{tot}}(0) = \hat{\rho}(0) \otimes \hat{\rho}_B(0)$
2. Born approximation: $\hat{\rho}_{\text{tot}}(\tau) \approx \hat{\rho}(\tau) \otimes \hat{\rho}_B(\tau)$
3. Invariance of the environment: $\hat{\rho}_B(\tau) \approx \hat{\rho}_B(0)$

By taking the noise average of (S17), we obtain

$$\frac{\partial}{\partial \tau} \hat{\rho}_I(\tau) = - \int_0^\tau d\tau' \text{Tr}_B \left\{ \left[\hat{V}_\eta(\tau), \left[\hat{V}_\eta(\tau'), \hat{\rho}_I(\tau') \otimes \hat{\rho}_B(0) \right] \right] \right\}, \quad (\text{S20})$$

where we use $\text{Tr}_B \{ \hat{\rho}_B(0) \} = 1$ and

$$\begin{aligned} \text{Tr}_B \left\{ \left[\hat{V}_\eta(\tau), \hat{\rho}_{\text{tot},I}(0) \right] \right\} &= \text{Tr}_B \{ \hat{\eta}(\tau) \hat{\rho}_B(0) \} \hat{L}^\dagger(\tau) \hat{\rho}(0) - \text{Tr}_B \{ \hat{\rho}_B(0) \hat{\eta}(\tau) \} \hat{\rho}(0) \hat{L}^\dagger(\tau) \\ &\quad + \text{Tr}_B \{ \hat{\eta}^\dagger(\tau) \hat{\rho}_B(0) \} \hat{L}(\tau) \hat{\rho}(0) - \text{Tr}_B \{ \hat{\rho}_B(0) \hat{\eta}^\dagger(\tau) \} \hat{\rho}(0) \hat{L}(\tau) \\ &= \langle \hat{\eta}(\tau) \rangle \hat{L}^\dagger(\tau) \hat{\rho}(0) - \langle \hat{\eta}(\tau) \rangle \hat{\rho}(0) \hat{L}^\dagger(\tau) \\ &\quad + \langle \hat{\eta}^\dagger(\tau) \rangle \hat{L}(\tau) \hat{\rho}(0) - \langle \hat{\eta}^\dagger(\tau) \rangle \hat{\rho}(0) \hat{L}(\tau) \\ &= 0. \end{aligned} \quad (\text{S21})$$

The above equation follows from the cyclic property of the trace $\text{Tr}_B \{ AB \} = \text{Tr}_B \{ BA \}$. The right hand side of Eq. (S20) is rewritten as

$$\begin{aligned} &\text{Tr}_B \left\{ \left[\hat{V}_\eta(\tau), \left[\hat{V}_\eta(\tau'), \hat{\rho}_I(\tau') \otimes \hat{\rho}_B(0) \right] \right] \right\} \\ &= \langle \hat{\eta}(\tau) \hat{\eta}^\dagger(\tau') \rangle_\eta \hat{L}^\dagger(\tau) \hat{L}(\tau') \hat{\rho}_I(\tau') + \langle \hat{\eta}(\tau') \hat{\eta}^\dagger(\tau) \rangle_\eta \hat{\rho}_I(\tau') \hat{L}^\dagger(\tau') \hat{L}(\tau) \\ &\quad - \langle \hat{\eta}(\tau') \hat{\eta}^\dagger(\tau) \rangle_\eta \hat{L}(\tau) \hat{\rho}_I(\tau') \hat{L}^\dagger(\tau') - \langle \hat{\eta}(\tau) \hat{\eta}^\dagger(\tau') \rangle_\eta \hat{L}(\tau') \hat{\rho}_I(\tau') \hat{L}^\dagger(\tau) \\ &= \gamma \delta(\tau - \tau') \left[\left\{ \hat{L}^\dagger(\tau) \hat{L}(\tau), \hat{\rho}_I(\tau) \right\} - 2 \hat{L}(\tau) \hat{\rho}_I(\tau) \hat{L}^\dagger(\tau) \right]. \end{aligned} \quad (\text{S22})$$

Finally, by using the following identity

$$\begin{aligned} \int_0^\tau d\tau' \delta(\tau - \tau') &= \int_{-\infty}^\tau d\tau' \delta(\tau - \tau') \quad (\delta(\tau) = 0 \text{ at } \tau \neq 0) \\ &= \int_0^\infty ds \delta(s) \quad (s = \tau - \tau') \\ &= \frac{1}{2} \int_{-\infty}^\infty ds \delta(s) \quad (\text{even function: } \delta(s) = \delta(-s)) \\ &= \frac{1}{2}, \end{aligned} \quad (\text{S23})$$

we obtain the Lindblad master equation in the interaction picture

$$\frac{\partial}{\partial \tau} \hat{\rho}_I(\tau) = \gamma \left[\hat{L}(\tau) \hat{\rho}_I(\tau) \hat{L}^\dagger(\tau) - \frac{\left\{ \hat{L}^\dagger(\tau) \hat{L}(\tau), \hat{\rho}_I(\tau) \right\}}{2} \right]. \quad (\text{S24})$$

Since the time derivative of the density matrix in the interaction picture is associated with that in the Schrödinger picture as follows:

$$\begin{aligned}\frac{\partial}{\partial\tau}\hat{\rho}_I(\tau) &= \frac{\partial}{\partial\tau}\left(e^{i(\hat{H}+\hat{H}_B)\tau}\hat{\rho}(\tau)e^{-i(\hat{H}+\hat{H}_B)\tau}\right) \\ &= e^{i(\hat{H}+\hat{H}_B)\tau}\left(\frac{\partial}{\partial\tau}\hat{\rho}(\tau) + i\left[\hat{H} + \hat{H}_B, \hat{\rho}(\tau)\right]\right)e^{-i(\hat{H}+\hat{H}_B)\tau} \\ &= e^{i(\hat{H}+\hat{H}_B)\tau}\left(\frac{\partial}{\partial\tau}\hat{\rho}(\tau) + i\left[\hat{H}, \hat{\rho}(\tau)\right]\right)e^{-i(\hat{H}+\hat{H}_B)\tau}.\end{aligned}\tag{S25}$$

we obtain the well-known Lindblad master equation

$$\frac{\partial}{\partial\tau}\hat{\rho}(\tau) = -i\left[\hat{H}, \hat{\rho}(\tau)\right] + \gamma\left[\hat{L}\hat{\rho}(\tau)\hat{L}^\dagger - \frac{\{\hat{L}^\dagger\hat{L}, \hat{\rho}(\tau)\}}{2}\right].\tag{S26}$$

It is instructive to clarify the assumptions underlying the above derivation. First, the initial separability between the system and the bath is a standard assumption in both quantum many-body and open quantum systems, allowing for a perturbative treatment. Second, the Born approximation presumes that this separability holds throughout the evolution, which is reasonable when the system-bath coupling is weak. Third, the time-invariance of the environment is naturally satisfied for a large bath in thermal equilibrium or in vacuum. In conventional derivations of the Lindblad master equation [1], the Markov and rotating-wave approximations are also imposed. In our case, however, these approximations are not explicitly required, as the Markov approximation is incorporated through the assumption of frequency-independent coupling in Eq. (S10), and the rotating-wave approximation is implemented via Eq. (S6).

It should also be emphasized that the Born approximation is essential for deriving Eqs. (S21) and (S22). Without this condition, Eq. (S13) cannot be applied directly, and the temporal correlations deviates from the delta function due to bath renormalization effects induced by the finite quantum system. This point is particularly suggestive when performing field-theoretic calculations based on Feynman diagram techniques, since perturbative expansions naturally generate diagrams corresponding to such bath renormalizations. To maintain consistency with the Lindblad master equation, it is necessary to discard these diagrams, a consideration that becomes especially crucial when analyzing two-body loss processes.

When the Lindblad operator \hat{L} involves two field operators, as in the case of two-particle loss, terms containing \hat{L} in Eq. (S26) effectively behave like interaction terms. The third term on the right-hand side of Eq. (S26) $-\gamma\{\hat{L}^\dagger\hat{L}, \hat{\rho}(t)\}/2$, corresponds to the so-called non-Hermitian evolution term and plays the role of an effective interaction with a complex amplitude in the context of two-body loss. The second term, $\gamma\hat{L}\hat{\rho}(t)\hat{L}^\dagger$, is referred to as the quantum jump term and is often omitted in non-Hermitian approaches to many-body physics. However, retaining this jump term is essential to ensure the completely-positive trace-preserving nature of the evolution of the density matrix. The noise-field formalism offers an alternative representation that consistently incorporates the full non-unitary dynamics described by Eq. (S26).

III. KELDYSH FORMALISM

In order to perform field-theoretic calculations, we now divide \hat{H} into an unperturbed part \hat{H}_0 and a perturbed part \hat{V} and construct the interaction picture of a system operator \hat{A}

$$\hat{A}_I(\tau) = e^{i(\hat{H}_0+\hat{H}_B)\tau}\hat{A}_S e^{-i(\hat{H}_0+\hat{H}_B)\tau},\tag{S27}$$

where the subscripts S and I denote the Schrödinger and interaction pictures. In the Keldysh formalism, we consider a contour-ordered Green's function of system operators \hat{A} and \hat{B} , which is defined on the contour illustrated in Fig. S1 and is given by

$$\begin{aligned}G^C(\tau, \tau') &= -i\left\langle T_C\left[\hat{A}_H(\tau)\hat{B}_H(\tau')\right]\right\rangle \\ &= \sum_{n=0}^{\infty}\frac{(-i)^{n+1}}{n!}\int_C d\tau_1\cdots\int_C d\tau_n\left\langle T_C\left[\left(\hat{V}_I(\tau_1)+\hat{V}_{\eta,I}(\tau_1)\right)\cdots\left(\hat{V}_I(\tau_n)+\hat{V}_{\eta,I}(\tau_n)\right)\hat{A}_I(\tau)\hat{B}_I(\tau')\right]\right\rangle_0.\end{aligned}\tag{S28}$$

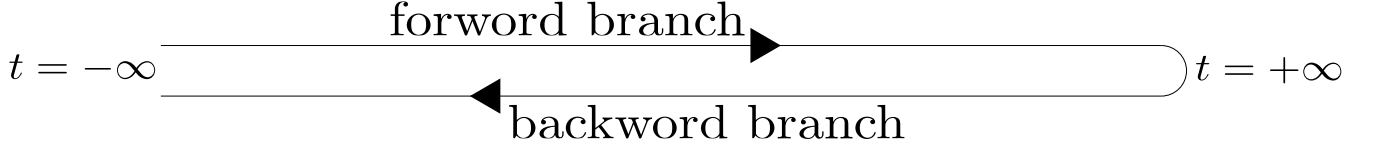


FIG. S1. Keldysh contour.

Here, the subscript H denotes the Heisenberg picture and $\langle \cdots \rangle_0$ is the unperturbed expectation value. In addition, T_C denotes contour-ordered product. When the \hat{H}_0 is bilinear in field operators, which holds in our system, Wick's theorem applies, and G^C can be computed by using a Dyson series expansion associated within the Feynman diagram technique.

In practical calculations of physical quantities, it is convenient to work with the retarded, advanced and Keldysh components of Green's functions. These components are related by the following expressions:

$$\begin{pmatrix} G^K(\tau, \tau') & G^R(\tau, \tau') \\ G^A(\tau, \tau') & 0 \end{pmatrix} = \begin{pmatrix} -i \langle [\hat{A}_H(\tau), \hat{B}_H(\tau')]_{\zeta} \rangle & -i\theta(\tau - \tau') \langle [\hat{A}_H(\tau), \hat{B}_H(\tau')]_{-\zeta} \rangle \\ i\theta(\tau' - \tau)\zeta \langle [\hat{A}_H(\tau), \hat{B}_H(\tau')]_{-\zeta} \rangle & 0 \end{pmatrix}, \quad (\text{S29})$$

$$\begin{pmatrix} G^T(\tau, \tau') & G^<(\tau, \tau') \\ G^>(\tau, \tau') & G^{\tilde{T}}(\tau, \tau') \end{pmatrix} = \begin{pmatrix} G^C(\tau^+, \tau'^+) & G^C(\tau^+, \tau'^-) \\ G^C(\tau^-, \tau'^+) & G^C(\tau^-, \tau'^-) \end{pmatrix} \quad (\text{S30})$$

$$= \begin{pmatrix} -i \langle T [\hat{A}_H(\tau) \hat{B}_H(\tau')] \rangle & -i \langle \hat{A}_H(\tau) \hat{B}_H(\tau') \rangle \\ -i\zeta \langle \hat{B}_H(\tau') \hat{A}_H(\tau) \rangle & -i \langle \tilde{T} [\hat{A}_H(\tau) \hat{B}_H(\tau')] \rangle \end{pmatrix} \quad (\text{S31})$$

$$= \frac{1}{2} \begin{pmatrix} G^K(\tau, \tau') + G^R(\tau, \tau') + G^A(\tau, \tau') & G^K(\tau, \tau') - G^R(\tau, \tau') + G^A(\tau, \tau') \\ G^K(\tau, \tau') + G^R(\tau, \tau') - G^A(\tau, \tau') & G^K(\tau, \tau') - G^R(\tau, \tau') - G^A(\tau, \tau') \end{pmatrix}. \quad (\text{S32})$$

Here, $\zeta = +1(-1)$ for bosons (fermions), $[A, B]_{\zeta} = AB + \zeta BA$. The time argument $\tau^{+(-)}$ denotes times on the forward (backward) branch of the Keldysh contour (see Fig. S1). The symbol $T(\tilde{T})$ denotes (anti-)time-ordered product, while $G^{<(>)}$ refers to lesser (greater) Green's function.

IV. FREQUENCY TUNING

In multi-terminal transport system, the origin of frequencies is defined by the average of reservoir's chemical potentials

$$\mu = \frac{\sum_i \mu_i}{\sum_i 1}, \quad (\text{S33})$$

where i denotes the reservoir i . When calculating reservoir's Green's functions, the distribution function of the reservoir i incorporates the energy shift depending on $\mu_i - \mu$. In this section, we review the method to compute this energy shift.

To elucidate the essential features, we focus on a two-terminal system. The typical expression of left (right) reservoir's Keldysh Green's function

$$g_{L(R)}^K(\mathbf{k}, \omega_{L(R)}) = -2\pi i \delta(\omega_{L(R)} - (\epsilon_{\mathbf{k}} - \mu_{L(R)})) n_{L(R)}(\omega_{L(R)}), \quad (\text{S34})$$

with $\epsilon_{\mathbf{k}} = \mathbf{k}^2/2m$ and $n_{L(R)}(\omega_{L(R)}) = \frac{1}{e^{\omega_{L(R)}/T_{L(R)} - \zeta}}$, implies that frequency $\omega_{L(R)}$ is measured from $\mu_{L(R)}$. When connecting left and right reservoirs with a quantum point contact, we measure the frequency ω from averaged chemical potential μ , and the energy shifts are considered as Fig. S2, leading to

$$\omega_{L/R} = \omega \mp \frac{\Delta\mu}{2}, \quad (\text{S35})$$

with $\Delta\mu = \mu_L - \mu_R$. Thus, we obtain

$$g_{L/R}^K(\mathbf{k}, \omega) = -2\pi i \delta((\omega \mp \Delta\mu/2) - \epsilon_{\mathbf{k}} - \mu_{L/R}) n_{L/R}(\omega), \quad (\text{S36})$$

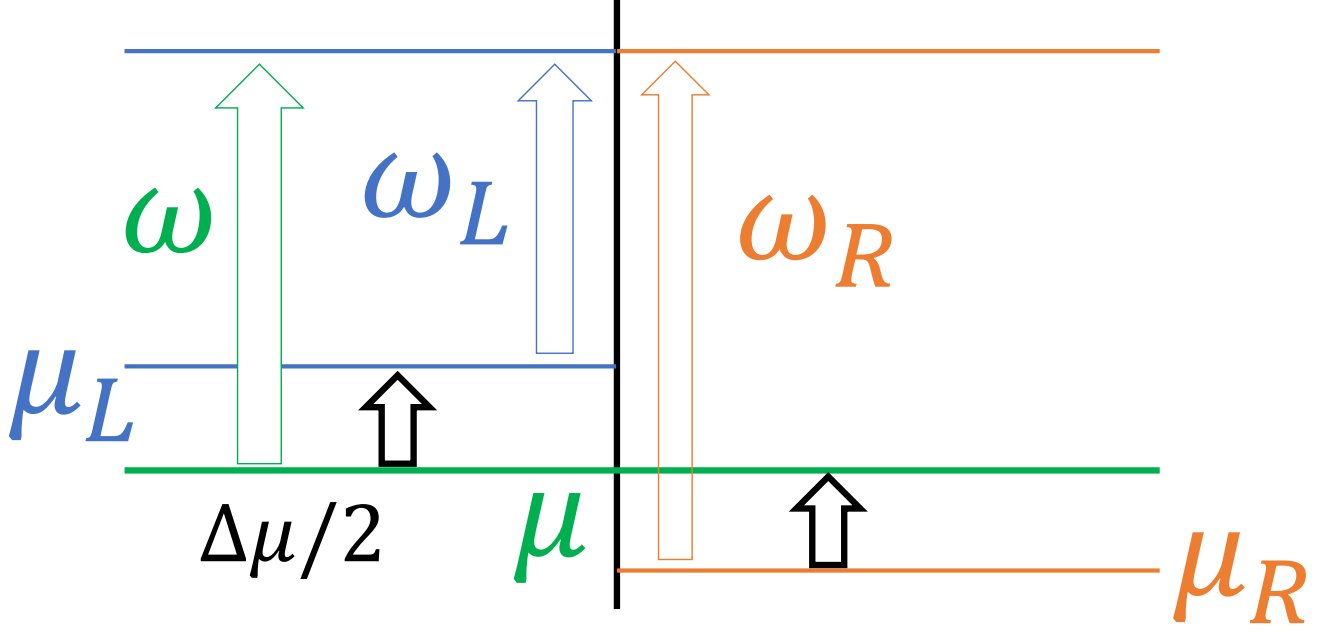


FIG. S2. Concept of frequency tuning.

with $n_{L/R}(\omega) = \frac{1}{e^{(\omega \mp \Delta\mu/2)/T_{L/R}} - \zeta}$.

To calculate the above results systematically, we start with the following canonical Hamiltonian

$$\hat{H} = \sum_{s=L,R} \sum_{\mathbf{k}} (\epsilon_{\mathbf{k}} - \mu) \hat{\psi}_{s\mathbf{k}}^\dagger \hat{\psi}_{s\mathbf{k}}, \quad (\text{S37})$$

where the energy is measured from μ . The system dynamics is described by \hat{H} while the equilibrium expectation value of Green's function (S36) is obtained by grand-canonical Hamiltonian

$$\hat{K} = \sum_{s=L,R} \sum_{\mathbf{k}} (\epsilon_{\mathbf{k}} - \mu_s) \hat{\psi}_{s\mathbf{k}}^\dagger \hat{\psi}_{s\mathbf{k}}. \quad (\text{S38})$$

Considering the difference between \hat{H} and \hat{K}

$$\hat{H}_\Delta = \hat{K} - \hat{H} = -\frac{\Delta\mu}{2} (\hat{N}_L - \hat{N}_R), \quad (\text{S39})$$

the annihilation operator of the interaction picture can be rewritten as

$$\hat{\psi}_{L/R\mathbf{k},I}(\tau) = e^{i\hat{H}\tau} \hat{\psi}_{L/R\mathbf{k},S} e^{-i\hat{H}\tau} \quad (\text{S40})$$

$$= e^{i\hat{K}\tau} e^{-i\hat{H}_\Delta\tau} \hat{\psi}_{L/R\mathbf{k},S} e^{i\hat{H}_\Delta\tau} e^{-i\hat{K}\tau} \quad (\text{S41})$$

$$= e^{\mp i\Delta\mu\tau/2} e^{i\hat{K}\tau} \hat{\psi}_{L/R\mathbf{k},S} e^{-i\hat{K}\tau} \quad (\text{S42})$$

$$\equiv e^{\mp i\Delta\mu\tau/2} \hat{\psi}_{L/R\mathbf{k},K}(\tau), \quad (\text{S43})$$

where the subscripts S, I and K denote the Schrödinger picture, the interaction picture constructed by \hat{H} , and the

interaction picture constructed by \hat{K} , respectively. Thus, we obtain

$$\left[g_{L/R}^C(\mathbf{k}, \tau, \tau') \right]_I \equiv -i \left\langle T_C \left[\hat{\psi}_{L/R\mathbf{k},I}(\tau) \hat{\psi}_{L/R\mathbf{k},I}^\dagger(\tau') \right] \right\rangle_0 \quad (\text{S44})$$

$$= -i \left\langle T_C \left[\hat{\psi}_{L/R\mathbf{k},K}(\tau) \hat{\psi}_{L/R\mathbf{k},K}^\dagger(\tau') \right] \right\rangle_0 e^{\mp i \Delta\mu(\tau-\tau')/2} \quad (\text{S45})$$

$$\equiv \left[g_{L/R}^C(\mathbf{k}, \tau, \tau') \right]_K e^{\mp i \Delta\mu(\tau-\tau')/2}, \quad (\text{S46})$$

where $[g]_{I(K)}$ is the Green's function constructed by $\hat{\psi}_{I(K)}$. When calculating the following integral, the expression of grand-canonical Hamiltonian is given by

$$\begin{aligned} & \int_{-\infty}^{\infty} d\tau_1 f(\tau, \tau_1) \left[g_{L/R}^K(\mathbf{k}, \tau_1, \tau') \right]_I \\ &= \int_{-\infty}^{\infty} d\tau_1 \int_{-\infty}^{\infty} \frac{d\omega}{2\pi} \int_{-\infty}^{\infty} \frac{d\omega_{L/R}}{2\pi} f(\omega) \left[g_{L/R}^K(\mathbf{k}, \omega_{L/R}) \right]_K e^{-i\omega(\tau-\tau_1)} e^{-i(\omega_{L/R} \pm \Delta\mu/2)(\tau_1-\tau')} \\ &= \int_{-\infty}^{\infty} \frac{d\omega}{2\pi} f(\omega) \left[g_{L/R}^K(\mathbf{k}, \omega \mp \Delta\mu/2) \right]_K e^{-i\omega(\tau-\tau')}, \end{aligned} \quad (\text{S47})$$

where f is a function which arises in the calculation, and $\left[g_{L/R}^K(\mathbf{k}, \omega \mp \Delta\mu/2) \right]_K$ corresponds Eq. (S36). The energy shifts of the retarded and advanced components of reservoir's Green's function can be obtained in the same manner.

V. ANALYSIS OF DEPHASING MODEL

To see how the noise field formalism works, we here analyze the dephasing model, which has also been examined in Refs. [2, 3]. For the sake of simplicity, we omit indices of site and spin. Then, the perturbed Hamiltonian is given by

$$\hat{V}_\eta = \hat{d}^\dagger \hat{d} \hat{\eta}. \quad (\text{S48})$$

Here, $\hat{d}(\hat{d}^\dagger)$ is an annihilation (creation) operator of the system and $\hat{\eta}$ is a real noise field, obeying the following condition:

$$\langle \hat{\eta}(\tau) \hat{\eta}(\tau') \rangle_\eta = \gamma \delta(\tau - \tau'), \quad \langle \hat{\eta}(\tau) \rangle_\eta = 0. \quad (\text{S49})$$

The contour-ordered Green's function satisfies

$$\begin{aligned} G^C(\tau, \tau') &= \sum_{n=0}^{\infty} \frac{(-i)^{n+1}}{n!} \int_C d\tau_1 \cdots \int_C d\tau_n \left\langle T_C \left[\hat{V}_\eta(\tau_1) \cdots \hat{V}_\eta(\tau_n) \hat{d}(\tau) \hat{d}^\dagger(\tau') \right] \right\rangle_0, \\ &= g^C(\tau, \tau') + \int_C d\tau_1 \int_C d\tau_2 g^C(\tau, \tau_1) \Sigma^C(\tau_1, \tau_2) G^C(\tau_2, \tau'), \end{aligned} \quad (\text{S50})$$

where g^C is an unperturbed Green's function and Σ^C is a self-energy.

In terms of Feynman diagrams, the coupling term (S48) is depicted as Fig. S3(a). Considering the noise average of pair of (S48), we obtain the Feynman diagram depicted in Fig. S3(b), which is similar to the diagram of the two-body interaction. A crucial difference between genuine interactions and Fig. S3(b) is that the latter connects time arguments on the forward and backward branches of the Keldysh contour while the former only connects time argument on the same branch.

We now examine typical diagrams of the dephasing model. For the crossing diagram shown in Fig. S4(a), the

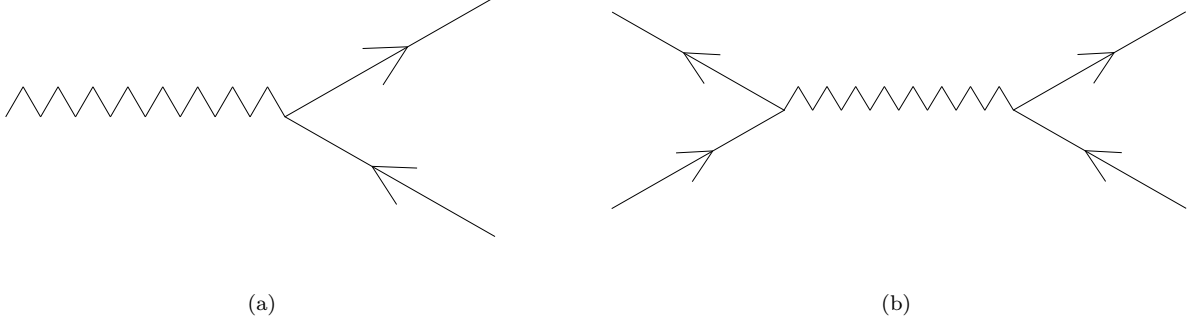


FIG. S3. (a) Feynman diagram corresponding to the coupling term (S48). The solid lines represent \hat{d} and \hat{d}^\dagger , and wavy line represents $\hat{\eta}$. (b) The term generated from the noise average of pair of (S48).

self-energy is given by

$$\begin{aligned}
\Sigma_{S4(a)}^T(\tau, \tau') &= \int_C d\tau_1 \int_C d\tau_2 A^C(\tau^+, \tau_1) B^C(\tau_1, \tau_2) C^C(\tau_2, \tau'^+) g_\eta^C(\tau^+, \tau_2) g_\eta^C(\tau_1, \tau'^+) \\
&= \int_{-\infty}^{\infty} d\tau_1 \int_{-\infty}^{\infty} d\tau_2 A^T(\tau, \tau_1) B^T(\tau_1, \tau_2) C^T(\tau_2, \tau') g_\eta^T(\tau, \tau_2) g_\eta^T(\tau_1, \tau') \\
&\quad - \int_{-\infty}^{\infty} d\tau_1 \int_{-\infty}^{\infty} d\tau_2 A^T(\tau, \tau_1) B^<(\tau_1, \tau_2) C^>(\tau_2, \tau') g_\eta^<(\tau, \tau_2) g_\eta^>(\tau_1, \tau') \\
&\quad - \int_{-\infty}^{\infty} d\tau_1 \int_{-\infty}^{\infty} d\tau_2 A^<(\tau, \tau_1) B^>(\tau_1, \tau_2) C^T(\tau_2, \tau') g_\eta^T(\tau, \tau_2) g_\eta^>(\tau_1, \tau') \\
&\quad + \int_{-\infty}^{\infty} d\tau_1 \int_{-\infty}^{\infty} d\tau_2 A^<(\tau, \tau_1) B^{\tilde{T}}(\tau_1, \tau_2) C^>(\tau_2, \tau') g_\eta^<(\tau, \tau_2) g_\eta^>(\tau_1, \tau') \\
&= -\gamma^2 A^T(\tau, \tau') \left[B^T(\tau', \tau) C^T(\tau, \tau') - B^<(\tau', \tau) C^>(\tau, \tau') \right] \\
&\quad - \gamma^2 A^<(\tau, \tau') \left[B^{\tilde{T}}(\tau', \tau) C^>(\tau, \tau') - B^>(\tau', \tau) C^T(\tau, \tau') \right],
\end{aligned} \tag{S51}$$

$$\begin{aligned}
\Sigma_{S4(a)}^<(\tau, \tau') &= \int_C d\tau_1 \int_C d\tau_2 A^C(\tau^+, \tau_1) B^C(\tau_1, \tau_2) C^C(\tau_2, \tau'^-) g_\eta^C(\tau^+, \tau_2) g_\eta^C(\tau_1, \tau'^-) \\
&= \int_{-\infty}^{\infty} d\tau_1 \int_{-\infty}^{\infty} d\tau_2 A^T(\tau, \tau_1) B^T(\tau_1, \tau_2) C^<(\tau_2, \tau') g_\eta^T(\tau, \tau_2) g_\eta^<(\tau_1, \tau') \\
&\quad - \int_{-\infty}^{\infty} d\tau_1 \int_{-\infty}^{\infty} d\tau_2 A^T(\tau, \tau_1) B^<(\tau_1, \tau_2) C^{\tilde{T}}(\tau_2, \tau') g_\eta^<(\tau, \tau_2) g_\eta^<(\tau_1, \tau') \\
&\quad - \int_{-\infty}^{\infty} d\tau_1 \int_{-\infty}^{\infty} d\tau_2 A^<(\tau, \tau_1) B^>(\tau_1, \tau_2) C^<(\tau_2, \tau') g_\eta^T(\tau, \tau_2) g_\eta^{\tilde{T}}(\tau_1, \tau') \\
&\quad + \int_{-\infty}^{\infty} d\tau_1 \int_{-\infty}^{\infty} d\tau_2 A^<(\tau, \tau_1) B^{\tilde{T}}(\tau_1, \tau_2) C^{\tilde{T}}(\tau_2, \tau') g_\eta^<(\tau, \tau_2) g_\eta^{\tilde{T}}(\tau_1, \tau') \\
&= -\gamma^2 A^T(\tau, \tau') \left[B^T(\tau', \tau) C^<(\tau, \tau') - B^<(\tau', \tau) C^{\tilde{T}}(\tau, \tau') \right] \\
&\quad - \gamma^2 A^<(\tau, \tau') \left[B^{\tilde{T}}(\tau', \tau) C^{\tilde{T}}(\tau, \tau') - B^>(\tau', \tau) C^<(\tau, \tau') \right],
\end{aligned} \tag{S52}$$

$$\begin{aligned}
\Sigma_{S4(a)}^>(\tau, \tau') &= \int_C d\tau_1 \int_C d\tau_2 A^C(\tau^-, \tau_1) B^C(\tau_1, \tau_2) C^C(\tau_2, \tau'^+) g_\eta^C(\tau^-, \tau_2) g_\eta^C(\tau_1, \tau'^+) \\
&= \int_{-\infty}^{\infty} d\tau_1 \int_{-\infty}^{\infty} d\tau_2 A^>(\tau, \tau_1) B^T(\tau_1, \tau_2) C^T(\tau_2, \tau') g_\eta^>(\tau, \tau_2) g_\eta^T(\tau_1, \tau') \\
&\quad - \int_{-\infty}^{\infty} d\tau_1 \int_{-\infty}^{\infty} d\tau_2 A^>(\tau, \tau_1) B^<(\tau_1, \tau_2) C^>(\tau_2, \tau') g_\eta^{\tilde{T}}(\tau, \tau_2) g_\eta^T(\tau_1, \tau') \\
&\quad - \int_{-\infty}^{\infty} d\tau_1 \int_{-\infty}^{\infty} d\tau_2 A^{\tilde{T}}(\tau, \tau_1) B^>(\tau_1, \tau_2) C^T(\tau_2, \tau') g_\eta^>(\tau, \tau_2) g_\eta^>(\tau_1, \tau') \\
&\quad + \int_{-\infty}^{\infty} d\tau_1 \int_{-\infty}^{\infty} d\tau_2 A^{\tilde{T}}(\tau, \tau_1) B^{\tilde{T}}(\tau_1, \tau_2) C^>(\tau_2, \tau') g_\eta^{\tilde{T}}(\tau, \tau_2) g_\eta^>(\tau_1, \tau') \\
&= -\gamma^2 A^>(\tau, \tau') \left[B^T(\tau', \tau) C^T(\tau, \tau') - B^<(\tau', \tau) C^>(\tau, \tau') \right] \\
&\quad - \gamma^2 A^{\tilde{T}}(\tau, \tau') \left[B^{\tilde{T}}(\tau', \tau) C^>(\tau, \tau') - B^>(\tau', \tau) C^T(\tau, \tau') \right],
\end{aligned} \tag{S53}$$

$$\begin{aligned}
\Sigma_{S4(a)}^{\tilde{T}}(\tau, \tau') &= \int_C d\tau_1 \int_C d\tau_2 A^C(\tau^-, \tau_1) B^C(\tau_1, \tau_2) C^C(\tau_2, \tau'^-) g_\eta^C(\tau^-, \tau_2) g_\eta^C(\tau_1, \tau'^-) \\
&= \int_{-\infty}^{\infty} d\tau_1 \int_{-\infty}^{\infty} d\tau_2 A^>(\tau, \tau_1) B^T(\tau_1, \tau_2) C^<(\tau_2, \tau') g_\eta^>(\tau, \tau_2) g_\eta^<(\tau_1, \tau') \\
&\quad - \int_{-\infty}^{\infty} d\tau_1 \int_{-\infty}^{\infty} d\tau_2 A^>(\tau, \tau_1) B^<(\tau_1, \tau_2) C^{\tilde{T}}(\tau_2, \tau') g_\eta^{\tilde{T}}(\tau, \tau_2) g_\eta^<(\tau_1, \tau') \\
&\quad - \int_{-\infty}^{\infty} d\tau_1 \int_{-\infty}^{\infty} d\tau_2 A^{\tilde{T}}(\tau, \tau_1) B^>(\tau_1, \tau_2) C^<(\tau_2, \tau') g_\eta^>(\tau, \tau_2) g_\eta^{\tilde{T}}(\tau_1, \tau') \\
&\quad + \int_{-\infty}^{\infty} d\tau_1 \int_{-\infty}^{\infty} d\tau_2 A^{\tilde{T}}(\tau, \tau_1) B^{\tilde{T}}(\tau_1, \tau_2) C^{\tilde{T}}(\tau_2, \tau') g_\eta^{\tilde{T}}(\tau, \tau_2) g_\eta^{\tilde{T}}(\tau_1, \tau') \\
&= -\gamma^2 A^>(\tau, \tau') \left[B^T(\tau', \tau) C^<(\tau, \tau') - B^<(\tau', \tau) C^{\tilde{T}}(\tau, \tau') \right] \\
&\quad - \gamma^2 A^{\tilde{T}}(\tau, \tau') \left[B^{\tilde{T}}(\tau', \tau) C^{\tilde{T}}(\tau, \tau') - B^>(\tau', \tau) C^<(\tau, \tau') \right],
\end{aligned} \tag{S54}$$

where

$$\begin{pmatrix} g_\eta^T(\tau, \tau') & g_\eta^<(\tau, \tau') \\ g_\eta^>(\tau, \tau') & g_\eta^{\tilde{T}}(\tau, \tau') \end{pmatrix} = \begin{pmatrix} -i \langle T[\hat{\eta}(\tau) \hat{\eta}(\tau')] \rangle_\eta & -i \langle \hat{\eta}(\tau) \hat{\eta}(\tau') \rangle_\eta \\ -i \langle \hat{\eta}(\tau') \hat{\eta}(\tau) \rangle_\eta & -i \langle \tilde{T}[\hat{\eta}(\tau) \hat{\eta}(\tau')] \rangle_\eta \end{pmatrix} = -i\gamma\delta(\tau - \tau') \begin{pmatrix} 1 & 1 \\ 1 & 1 \end{pmatrix} \tag{S55}$$

with $\theta(0) = 1/2$. Using the relations of each component (S32), we obtain

$$\begin{aligned}
\Sigma_{S4(a)}^K(\tau, \tau') &= \frac{1}{2} \left(\Sigma^T(\tau, \tau') + \Sigma^<(\tau, \tau') + \Sigma^>(\tau, \tau') + \Sigma^{\tilde{T}}(\tau, \tau') \right) \\
&= -\gamma^2 \left(A^R(\tau, \tau') B^R(\tau', \tau) C^K(\tau, \tau') + A^R(\tau, \tau') B^K(\tau', \tau) C^A(\tau, \tau') + A^K(\tau, \tau') B^A(\tau', \tau) C^A(\tau, \tau') \right) \\
&= 0,
\end{aligned} \tag{S56}$$

$$\begin{aligned}
\Sigma_{S4(a)}^R(\tau, \tau') &= \frac{1}{2} \left(\Sigma^T(\tau, \tau') - \Sigma^<(\tau, \tau') + \Sigma^>(\tau, \tau') - \Sigma^{\tilde{T}}(\tau, \tau') \right) \\
&= -\gamma^2 A^R(\tau, \tau') B^R(\tau', \tau) C^R(\tau, \tau') \\
&= 0,
\end{aligned} \tag{S57}$$

$$\begin{aligned}
\Sigma_{S4(a)}^A(\tau, \tau') &= \frac{1}{2} \left(\Sigma^T(\tau, \tau') + \Sigma^<(\tau, \tau') - \Sigma^>(\tau, \tau') - \Sigma^{\tilde{T}}(\tau, \tau') \right) \\
&= -\gamma^2 A^A(\tau, \tau') B^A(\tau', \tau) C^A(\tau, \tau') \\
&= 0,
\end{aligned} \tag{S58}$$

with the causality $A^R(\tau, \tau') B^R(\tau', \tau) = B^A(\tau', \tau) C^A(\tau, \tau') = A^R(\tau, \tau') C^A(\tau, \tau') = 0$ in the integral of Eq. (S50). Thus, the crossing diagram is shown to vanish.

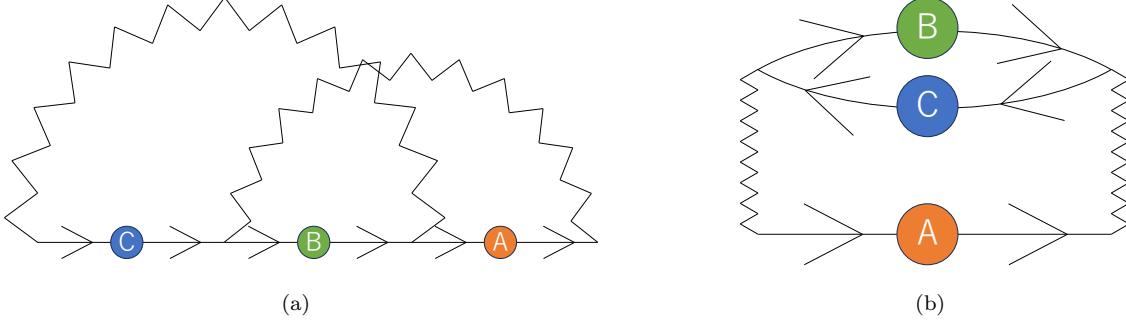


FIG. S4. (a) Self-energy of the crossing diagram. (b) Diagram associated with bath renormalization by \hat{d} and \hat{d}^\dagger .

We next consider the diagram shown in Fig. S4(b), representing the effective renormalization of the noise field properties by the fields of the system \hat{d} and \hat{d}^\dagger . As in the case of the crossing diagram, the self-energy is given by

$$\begin{aligned}
 \Sigma_{S4(b)}^T(\tau, \tau') &= \int_C d\tau_1 \int_C d\tau_2 A^C(\tau^+, \tau'^+) B^C(\tau_1, \tau_2) C^C(\tau_2, \tau_1) g_\eta^C(\tau^+, \tau_1) g_\eta^C(\tau_2, \tau'^+) \\
 &= \int_{-\infty}^{\infty} d\tau_1 \int_{-\infty}^{\infty} d\tau_2 A^T(\tau, \tau') B^T(\tau_1, \tau_2) C^T(\tau_2, \tau_1) g_\eta^T(\tau, \tau_1) g_\eta^T(\tau_2, \tau') \\
 &\quad - \int_{-\infty}^{\infty} d\tau_1 \int_{-\infty}^{\infty} d\tau_2 A^T(\tau, \tau') B^<(\tau_1, \tau_2) C^>(\tau_2, \tau_1) g_\eta^T(\tau, \tau_1) g_\eta^>(\tau_2, \tau') \\
 &\quad - \int_{-\infty}^{\infty} d\tau_1 \int_{-\infty}^{\infty} d\tau_2 A^T(\tau, \tau') B^>(\tau_1, \tau_2) C^<(\tau_2, \tau_1) g_\eta^<(\tau, \tau_1) g_\eta^T(\tau_2, \tau') \\
 &\quad + \int_{-\infty}^{\infty} d\tau_1 \int_{-\infty}^{\infty} d\tau_2 A^T(\tau, \tau') B^{\tilde{T}}(\tau_1, \tau_2) C^{\tilde{T}}(\tau_2, \tau_1) g_\eta^<(\tau, \tau_1) g_\eta^>(\tau_2, \tau') \\
 &= -\gamma^2 A^T(\tau, \tau') \left[B^T(\tau, \tau') C^T(\tau', \tau) - B^<(\tau, \tau') C^>(\tau', \tau) - B^>(\tau, \tau') C^<(\tau', \tau) + B^{\tilde{T}}(\tau, \tau') C^{\tilde{T}}(\tau', \tau) \right],
 \end{aligned} \tag{S59}$$

$$\begin{aligned}
 \Sigma_{S4(b)}^<(\tau, \tau') &= \int_C d\tau_1 \int_C d\tau_2 A^C(\tau^+, \tau'^-) B^C(\tau_1, \tau_2) C^C(\tau_2, \tau_1) g_\eta^C(\tau^+, \tau_1) g_\eta^C(\tau_2, \tau'^-) \\
 &= \int_{-\infty}^{\infty} d\tau_1 \int_{-\infty}^{\infty} d\tau_2 A^<(\tau, \tau') B^T(\tau_1, \tau_2) C^T(\tau_2, \tau_1) g_\eta^<(\tau, \tau_1) g_\eta^<(\tau_2, \tau') \\
 &\quad - \int_{-\infty}^{\infty} d\tau_1 \int_{-\infty}^{\infty} d\tau_2 A^<(\tau, \tau') B^<(\tau_1, \tau_2) C^>(\tau_2, \tau_1) g_\eta^<(\tau, \tau_1) g_\eta^{\tilde{T}}(\tau_2, \tau') \\
 &\quad - \int_{-\infty}^{\infty} d\tau_1 \int_{-\infty}^{\infty} d\tau_2 A^<(\tau, \tau') B^>(\tau_1, \tau_2) C^<(\tau_2, \tau_1) g_\eta^<(\tau, \tau_1) g_\eta^<(\tau_2, \tau') \\
 &\quad + \int_{-\infty}^{\infty} d\tau_1 \int_{-\infty}^{\infty} d\tau_2 A^<(\tau, \tau') B^{\tilde{T}}(\tau_1, \tau_2) C^{\tilde{T}}(\tau_2, \tau_1) g_\eta^<(\tau, \tau_1) g_\eta^{\tilde{T}}(\tau_2, \tau') \\
 &= -\gamma^2 A^<(\tau, \tau') \left[B^T(\tau, \tau') C^T(\tau', \tau) - B^<(\tau, \tau') C^>(\tau', \tau) - B^>(\tau, \tau') C^<(\tau', \tau) + B^{\tilde{T}}(\tau, \tau') C^{\tilde{T}}(\tau', \tau) \right],
 \end{aligned} \tag{S60}$$

$$\begin{aligned}
& \Sigma_{S4(b)}^>(\tau, \tau') \\
&= \int_C d\tau_1 \int_C d\tau_2 A^C(\tau^-, \tau'^+) B^C(\tau_1, \tau_2) C^C(\tau_2, \tau_1) g_\eta^C(\tau^-, \tau_1) g_\eta^C(\tau_2, \tau'^+) \\
&= \int_{-\infty}^{\infty} d\tau_1 \int_{-\infty}^{\infty} d\tau_2 A^>(\tau, \tau') B^T(\tau_1, \tau_2) C^T(\tau_2, \tau_1) g_\eta^>(\tau, \tau_1) g_\eta^T(\tau_2, \tau') \\
&\quad - \int_{-\infty}^{\infty} d\tau_1 \int_{-\infty}^{\infty} d\tau_2 A^>(\tau, \tau') B^<(\tau_1, \tau_2) C^>(\tau_2, \tau_1) g_\eta^>(\tau, \tau_1) g_\eta^>(\tau_2, \tau') \\
&\quad - \int_{-\infty}^{\infty} d\tau_1 \int_{-\infty}^{\infty} d\tau_2 A^>(\tau, \tau') B^>(\tau_1, \tau_2) C^<(\tau_2, \tau_1) g_\eta^{\tilde{T}}(\tau, \tau_1) g_\eta^T(\tau_2, \tau') \\
&\quad + \int_{-\infty}^{\infty} d\tau_1 \int_{-\infty}^{\infty} d\tau_2 A^>(\tau, \tau') B^{\tilde{T}}(\tau_1, \tau_2) C^{\tilde{T}}(\tau_2, \tau_1) g_\eta^{\tilde{T}}(\tau, \tau_1) g_\eta^>(\tau_2, \tau') \\
&= -\gamma^2 A^>(\tau, \tau') \left[B^T(\tau, \tau') C^T(\tau', \tau) - B^<(\tau, \tau') C^>(\tau', \tau) - B^>(\tau, \tau') C^<(\tau', \tau) + B^{\tilde{T}}(\tau, \tau') C^{\tilde{T}}(\tau', \tau) \right],
\end{aligned} \tag{S61}$$

$$\begin{aligned}
& \Sigma_{S4(b)}^{\tilde{T}}(\tau, \tau') \\
&= \int_C d\tau_1 \int_C d\tau_2 A^C(\tau^-, \tau'^-) B^C(\tau_1, \tau_2) C^C(\tau_2, \tau_1) g_\eta^C(\tau^-, \tau_1) g_\eta^C(\tau_2, \tau'^-) \\
&= \int_{-\infty}^{\infty} d\tau_1 \int_{-\infty}^{\infty} d\tau_2 A^{\tilde{T}}(\tau, \tau') B^T(\tau_1, \tau_2) C^T(\tau_2, \tau_1) g_\eta^>(\tau, \tau_1) g_\eta^<(\tau_2, \tau') \\
&\quad - \int_{-\infty}^{\infty} d\tau_1 \int_{-\infty}^{\infty} d\tau_2 A^{\tilde{T}}(\tau, \tau') B^<(\tau_1, \tau_2) C^>(\tau_2, \tau_1) g_\eta^>(\tau, \tau_1) g_\eta^{\tilde{T}}(\tau_2, \tau') \\
&\quad - \int_{-\infty}^{\infty} d\tau_1 \int_{-\infty}^{\infty} d\tau_2 A^{\tilde{T}}(\tau, \tau') B^>(\tau_1, \tau_2) C^<(\tau_2, \tau_1) g_\eta^{\tilde{T}}(\tau, \tau_1) g_\eta^<(\tau_2, \tau') \\
&\quad + \int_{-\infty}^{\infty} d\tau_1 \int_{-\infty}^{\infty} d\tau_2 A^{\tilde{T}}(\tau, \tau') B^{\tilde{T}}(\tau_1, \tau_2) C^{\tilde{T}}(\tau_2, \tau_1) g_\eta^{\tilde{T}}(\tau, \tau_1) g_\eta^{\tilde{T}}(\tau_2, \tau') \\
&= -\gamma^2 A^{\tilde{T}}(\tau, \tau') \left[B^T(\tau, \tau') C^T(\tau', \tau) - B^<(\tau, \tau') C^>(\tau', \tau) - B^>(\tau, \tau') C^<(\tau', \tau) + B^{\tilde{T}}(\tau, \tau') C^{\tilde{T}}(\tau', \tau) \right].
\end{aligned} \tag{S62}$$

Thus, we obtain

$$\Sigma_{S4(b)}^K(\tau, \tau') = A^K(\tau, \tau') \left(B^R(\tau, \tau') C^R(\tau', \tau) + B^A(\tau, \tau') C^A(\tau', \tau) \right) = 0, \tag{S63}$$

$$\Sigma_{S4(b)}^R(\tau, \tau') = A^R(\tau, \tau') \left(B^R(\tau, \tau') C^R(\tau', \tau) + B^A(\tau, \tau') C^A(\tau', \tau) \right) = 0, \tag{S64}$$

$$\Sigma_{S4(b)}^A(\tau, \tau') = A^A(\tau, \tau') \left(B^R(\tau, \tau') C^R(\tau', \tau) + B^A(\tau, \tau') C^A(\tau', \tau) \right) = 0. \tag{S65}$$

Thus, it turns out that the bath renormalization does not appear. We note that the absence of the bath renormalization is a particular feature in the dephasing model, and is not expected in the case of two-body loss.

The above lessons imply that a number of diagrams in the dephasing model vanish due to causality and symmetry of noise Green's functions, namely, $g_\eta^T(\tau, \tau') = g_\eta^<(\tau, \tau') = g_\eta^>(\tau, \tau') = g_\eta^{\tilde{T}}(\tau, \tau')$. At the end of the day, the remaining diagrams in the dephasing model is ones corresponding to the self-consistent Born approximation (SCBA) whose the Feynman diagram is shown in Fig. S6. By using the symmetry of noise Green's functions, the self-energy of the SCBA is obtained as

$$\Sigma^C(\tau, \tau') = i g_\eta^C(\tau, \tau') G^C(\tau, \tau'). \tag{S66}$$

From the lessons of the dephasing model, we can claim why genuine interactions cannot be solved exactly. As in the case of the noise-field formalism, we can introduce auxiliary fields for genuine interactions by assuming $g^<(\tau, \tau') = g^>(\tau, \tau') = 0$ for auxiliary fields. Under this condition, however, auxiliary-field Green's functions do not show symmetric properties unlike noise-field Green's functions in the dephasing model. For this reason, cancellation of a number of Feynman diagrams is not expected in generic many-body systems.

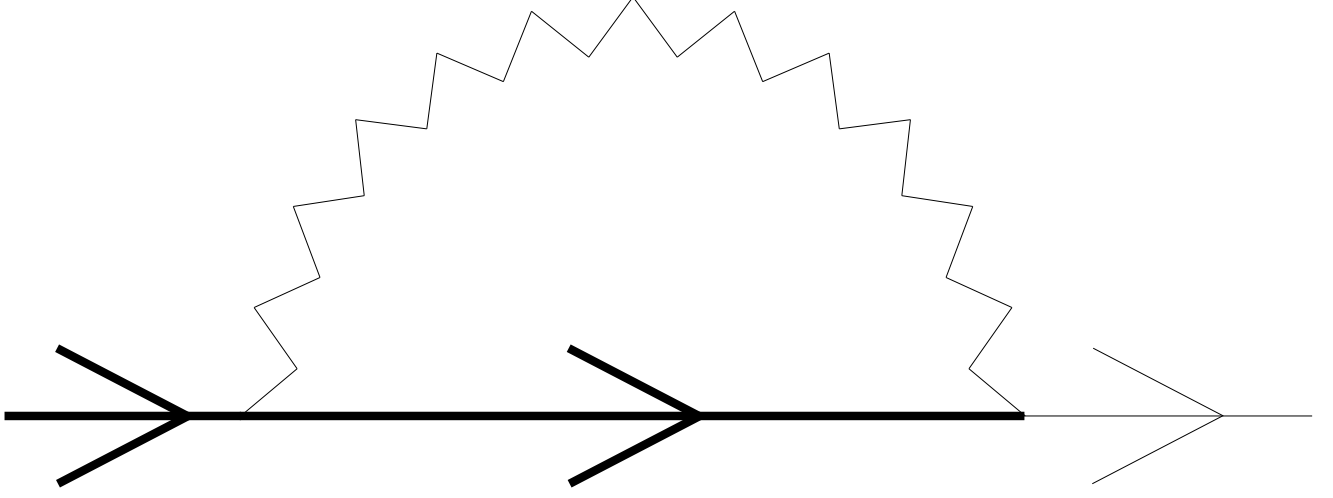


FIG. S5. Feynman diagram corresponding to the SCBA in the dephasing model.

VI. TWO-PARTICLE LOSS: SINGLE-SITE CASE

In this section, we derive the technical details of the main text by focusing on the single-site case. The Hamiltonian of the system is

$$H = \sum_{s=L,R} \sum_{\sigma=\uparrow,\downarrow} H_{s\sigma} + H_T + H_{1D}^0, \quad (\text{S67})$$

where

$$H_{s\sigma} = \sum_{\mathbf{k}} (\epsilon_{\mathbf{k}} - \mu_{s\sigma}) \psi_{s\mathbf{k}\sigma}^\dagger \psi_{s\mathbf{k}\sigma}, \quad (\text{S68})$$

$$H_T = - \sum_{s\mathbf{k}\sigma} \left(t_{\mathbf{k}} \psi_{s\mathbf{k}\sigma}^\dagger d_{0\sigma} + t_{\mathbf{k}}^* d_{0\sigma}^\dagger \psi_{s\mathbf{k}\sigma} \right), \quad (\text{S69})$$

$$H_{1D}^0 = \sum_{\sigma} \epsilon_0 d_{0\sigma}^\dagger d_{0\sigma}. \quad (\text{S70})$$

We now turn to the general form and introduce the noise field term

$$V_\eta = d_{0\uparrow}^\dagger d_{0\downarrow}^\dagger \eta + \eta^\dagger d_{0\downarrow} d_{0\uparrow}. \quad (\text{S71})$$

To obtain the same results as those obtained by the Lindblad master equation, we impose the following conditions:

$$\langle \eta(\tau) \eta^\dagger(\tau') \rangle_\eta = \gamma \delta(\tau - \tau'), \quad \langle \eta^\dagger(\tau) \eta(\tau') \rangle_\eta = \langle \eta(\tau) \eta(\tau') \rangle_\eta = \langle \eta^\dagger(\tau) \eta^\dagger(\tau') \rangle_\eta = \langle \eta(\tau) \rangle_\eta = \langle \eta^\dagger(\tau) \rangle_\eta = 0. \quad (\text{S72})$$

Current operators are then given by

$$I_{s\sigma} = - \frac{\partial}{\partial \tau} N_{s\sigma} = -i [H_{\text{tot}}, N_{s\sigma}] = -i [H_T, N_{s\sigma}] = -i \sum_{\mathbf{k}} \left(t_{\mathbf{k}} \psi_{s\mathbf{k}\sigma}^\dagger d_{0\sigma} - t_{\mathbf{k}}^* d_{0\sigma}^\dagger \psi_{s\mathbf{k}\sigma} \right), \quad (\text{S73})$$

$$I_{E,s\sigma} = - \frac{\partial}{\partial \tau} (H_{s\sigma} + \mu_{s\sigma} N_{s\sigma}) = -i \sum_{\mathbf{k}} \epsilon_{\mathbf{k}} \left(t_{\mathbf{k}} \psi_{s\mathbf{k}\sigma}^\dagger d_{0\sigma} - t_{\mathbf{k}}^* d_{0\sigma}^\dagger \psi_{s\mathbf{k}\sigma} \right). \quad (\text{S74})$$

The expectation values of current operators are expressed as follows:

$$\langle I_{s\sigma} \rangle = \zeta \sum_{\mathbf{k}} \text{Re} \left[t_{\mathbf{k}} G_{ds\sigma}^K(\mathbf{k}, \tau, \tau) \right] = \zeta \int \frac{d\omega}{2\pi} \sum_{\mathbf{k}} \text{Re} \left[t_{\mathbf{k}} G_{ds\sigma}^K(\mathbf{k}, \omega) \right], \quad (\text{S75})$$

$$\langle I_{E,s\sigma} \rangle = \zeta \sum_{\mathbf{k}} \epsilon_{\mathbf{k}} \text{Re} \left[t_{\mathbf{k}} G_{ds\sigma}^K(\mathbf{k}, \tau, \tau) \right] = \zeta \int \frac{d\omega}{2\pi} \sum_{\mathbf{k}} \epsilon_{\mathbf{k}} \text{Re} \left[t_{\mathbf{k}} G_{ds\sigma}^K(\mathbf{k}, \omega) \right], \quad (\text{S76})$$

where

$$G_{ds\sigma}^K(\mathbf{k}, \tau, \tau') = -i \left\langle \left[d_{0\sigma}(\tau), \psi_{s\mathbf{k}\sigma}^\dagger(\tau') \right] \right\rangle_\zeta. \quad (\text{S78})$$

To calculate the Green's function $G_{s\sigma}^K$, we construct the interaction picture by treating $H_T + V_\eta$ as a perturbation, and we calculate $G_{ds\sigma}^K$ by Wick expansion

$$\begin{aligned} G_{ds\sigma}^C(\mathbf{k}, \tau, \tau') &= -i \left\langle T_C \left[d_{0\sigma}(\tau) \psi_{s\mathbf{k}\sigma}^\dagger(\tau') \right] \right\rangle \\ &= \sum_{n=0}^{\infty} \frac{(-i)^{n+1}}{n!} \int_C d\tau_1 \cdots \int_C d\tau_n \left\langle T_C \left[\{H_T(\tau_1) + V_\eta(\tau_1)\} \cdots \{H_T(\tau_n) + V_\eta(\tau_n)\} d_{0\sigma}(\tau) \psi_{s\mathbf{k}\sigma}^\dagger(\tau') \right] \right\rangle_0 \\ &= g_{ds\sigma}^C(\mathbf{k}, \tau, \tau') \\ &\quad + \sum_{n=1}^{\infty} \frac{(-i)^{n+1}}{n!} \int_C d\tau_1 \cdots \int_C d\tau_n \sum_{j=1}^n \sum_{s_j \mathbf{k}_j \sigma_j} (-t_{\mathbf{k}_j}^*) \delta_{ss_j} \delta_{\mathbf{k}\mathbf{k}_j} \delta_{\sigma\sigma_j} g_{s\sigma}^C(\mathbf{k}, \tau_j, \tau') \\ &\quad \times \left\langle T_C \left[\{H_T(\tau_1) + V_\eta(\tau_1)\} \cdots \{H_T(\tau_n) + V_\eta(\tau_n)\} d_{0\sigma}(\tau) d_{0\sigma_j}^\dagger(\tau_j) \right] \right\rangle_0, \end{aligned} \quad (\text{S79})$$

where

$$g_{ds\sigma}^C(\mathbf{k}, \tau, \tau') = -i \left\langle T_C \left[d_{0\sigma}(\tau) \psi_{s\mathbf{k}\sigma}^\dagger(\tau') \right] \right\rangle_0 = 0, \quad (\text{S80})$$

$$-i \left\langle T_C \left[\psi_{s_j \mathbf{k}_j \sigma_j}^\dagger(\tau_j) \psi_{s\mathbf{k}\sigma}^\dagger(\tau') \right] \right\rangle_0 = -i \left\langle T_C \left[\psi_{s\mathbf{k}\sigma}^\dagger(\tau_j) \psi_{s\mathbf{k}\sigma}^\dagger(\tau') \right] \right\rangle_0 \delta_{ss_j} \delta_{\mathbf{k}\mathbf{k}_j} \delta_{\sigma\sigma_j} = g_{s\sigma}^C(\mathbf{k}, \tau_j, \tau') \delta_{ss_j} \delta_{\mathbf{k}\mathbf{k}_j} \delta_{\sigma\sigma_j}. \quad (\text{S81})$$

The contribution of each j is equal and the Green's function is given by

$$G_{ds\sigma}^C(\mathbf{k}, \tau, \tau') = \sum_{n=1}^{\infty} \frac{(-i)^{n+1}}{n!} \int_C d\tau_1 \cdots \int_C d\tau_n (-t_{\mathbf{k}}^*) \sum_{j=1}^n g_{s\sigma}^C(\mathbf{k}, \tau_j, \tau') \quad (\text{S82})$$

$$\times \left\langle T_C \left[\{H_T(\tau_1) + V_\eta(\tau_1)\} \cdots \{H_T(\tau_n) + V_\eta(\tau_n)\} d_{0\sigma}(\tau) d_{0\sigma_j}^\dagger(\tau_j) \right] \right\rangle_0 \quad (\text{S83})$$

$$= \sum_{n=1}^{\infty} \frac{(-i)^{n+1}}{n!} \int_C d\tau_1 \cdots \int_C d\tau_n (-t_{\mathbf{k}}^*) \sum_{j=1}^n g_{s\sigma}^C(\mathbf{k}, \tau'', \tau') \quad (\text{S84})$$

$$\times \left\langle T_C \left[\{H_T(\tau_1) + V_\eta(\tau_1)\} \cdots \{H_T(\tau_n) + V_\eta(\tau_n)\} d_{0\sigma}(\tau) d_{0\sigma_j}^\dagger(\tau'') \right] \right\rangle_0 \quad (\text{S85})$$

$$= -t_{\mathbf{k}}^* \int_C d\tau'' G_{11\sigma}^C(\tau, \tau'') g_{s\sigma}^C(\mathbf{k}, \tau'', \tau'), \quad (\text{S86})$$

where

$$G_{11\sigma}^C(\tau, \tau') = -i \left\langle T_C \left[d_{0\sigma}(\tau) d_{0\sigma}^\dagger(\tau') \right] \right\rangle \quad (\text{S87})$$

$$= \sum_{n=0}^{\infty} \frac{(-i)^{n+1}}{n!} \int_C d\tau_1 \cdots \int_C d\tau_n \left\langle T_C \left[\{H_T(\tau_1) + V_\eta(\tau_1)\} \cdots \{H_T(\tau_n) + V_\eta(\tau_n)\} d_{0\sigma}(\tau) d_{0\sigma}^\dagger(\tau') \right] \right\rangle_0. \quad (\text{S88})$$

The Green's function $G_{11\sigma}^C$ corresponds $G_{\frac{M+1}{2}\frac{M+1}{2}\sigma}^C$ in the multi-site case. By using the Langreth rule

$$G_{ds\sigma}^K(\mathbf{k}, \tau, \tau') = -t_{\mathbf{k}}^* \int_C d\tau'' \left(G_{11\sigma}^R(\tau, \tau'') g_{s\sigma}^K(\mathbf{k}, \tau'', \tau') + G_{11\sigma}^K(\tau, \tau'') g_{s\sigma}^A(\mathbf{k}, \tau'', \tau') \right), \quad (\text{S89})$$

we obtain

$$\begin{aligned} \langle I_{s\sigma} \rangle &= -\zeta \int d\tau' \sum_{\mathbf{k}} |t_{\mathbf{k}}|^2 \text{Re} \left[G_{11\sigma}^R(\tau, \tau') g_{s\sigma}^K(\mathbf{k}, \tau', \tau) + G_{11\sigma}^K(\tau, \tau') g_{s\sigma}^A(\mathbf{k}, \tau', \tau) \right] \\ &= -\zeta \int \frac{d\omega}{2\pi} \sum_{\mathbf{k}} |t_{\mathbf{k}}|^2 \text{Re} \left[G_{11\sigma}^R(\omega) g_{s\sigma}^K(\mathbf{k}, \omega) + G_{11\sigma}^K(\omega) g_{s\sigma}^A(\mathbf{k}, \omega) \right], \end{aligned} \quad (\text{S90})$$

$$\begin{aligned} \langle I_{E,s\sigma} \rangle &= -\zeta \int d\tau' \sum_{\mathbf{k}} \epsilon_{\mathbf{k}} |t_{\mathbf{k}}|^2 \text{Re} \left[G_{11\sigma}^R(\tau, \tau') g_{s\sigma}^K(\mathbf{k}, \tau', \tau) + G_{11\sigma}^K(\tau, \tau') g_{s\sigma}^A(\mathbf{k}, \tau', \tau) \right] \\ &= -\zeta \int \frac{d\omega}{2\pi} \sum_{\mathbf{k}} \epsilon_{\mathbf{k}} |t_{\mathbf{k}}|^2 \text{Re} \left[G_{11\sigma}^R(\omega) g_{s\sigma}^K(\mathbf{k}, \omega) + G_{11\sigma}^K(\omega) g_{s\sigma}^A(\mathbf{k}, \omega) \right]. \end{aligned} \quad (\text{S91})$$

To calculate $G_{11\sigma}^C$, we first eliminate the degree of freedom $\psi_{s\mathbf{k}\sigma}$. One of the simplest way to achieve it is to adopt the path integral representation of the partition function [4]. Since the reservoir action is bilinear in $\psi_{s\mathbf{k}\sigma}$, we can exactly integrate out the reservoir degrees of freedom as follows:

$$\begin{aligned} &\int \mathcal{D}[\bar{\psi}_{s\mathbf{k}\sigma}, \psi_{s\mathbf{k}\sigma}] \exp \left[- \int \frac{d\omega}{2\pi} \sum_{s\mathbf{k}} \begin{pmatrix} \bar{\psi}_{s\mathbf{k}\sigma}^{cl} & \bar{\psi}_{s\mathbf{k}\sigma}^q \end{pmatrix} \begin{pmatrix} 0 & -i[g_{s\sigma}^{-1}(\mathbf{k}, \omega)]^A \\ -i[g_{s\sigma}^{-1}(\mathbf{k}, \omega)]^R & -i[g_{s\sigma}^{-1}(\mathbf{k}, \omega)]^K \end{pmatrix} \begin{pmatrix} \psi_{s\mathbf{k}\sigma}^{cl} \\ \psi_{s\mathbf{k}\sigma}^q \end{pmatrix} \right] \\ &\times \exp \left[\int \frac{d\omega}{2\pi} \sum_{s\mathbf{k}} \begin{pmatrix} \bar{\psi}_{s\mathbf{k}\sigma}^{cl} & \bar{\psi}_{s\mathbf{k}\sigma}^q \end{pmatrix} i t_{\mathbf{k}} \hat{\sigma}_1 \begin{pmatrix} d_{\sigma}^{cl} \\ d_{\sigma}^q \end{pmatrix} + \int \frac{d\omega}{2\pi} \sum_{s\mathbf{k}} \begin{pmatrix} \bar{d}_{\sigma}^{cl} & \bar{d}_{\sigma}^q \end{pmatrix} i t_{\mathbf{k}}^* \hat{\sigma}_1 \begin{pmatrix} \psi_{s\mathbf{k}\sigma}^{cl} \\ \psi_{s\mathbf{k}\sigma}^q \end{pmatrix} \right] \\ &= \exp \left[\int \frac{d\omega}{2\pi} \sum_{s\mathbf{k}} \begin{pmatrix} \bar{d}_{\sigma}^{cl} & \bar{d}_{\sigma}^q \end{pmatrix} i t_{\mathbf{k}}^* \hat{\sigma}_1 \begin{pmatrix} i g_{s\sigma}^K(\mathbf{k}, \omega) & i g_{s\sigma}^R(\mathbf{k}, \omega) \\ i g_{s\sigma}^A(\mathbf{k}, \omega) & 0 \end{pmatrix} i t_{\mathbf{k}} \hat{\sigma}_1 \begin{pmatrix} d_{\sigma}^{cl} \\ d_{\sigma}^q \end{pmatrix} \right] \\ &= \exp \left[-i \int \frac{d\omega}{2\pi} \begin{pmatrix} \bar{d}_{\sigma}^{cl} & \bar{d}_{\sigma}^q \end{pmatrix} \sum_{\mathbf{k}s} |t_{\mathbf{k}}|^2 \begin{pmatrix} 0 & g_{s\sigma}^A(\mathbf{k}, \omega) \\ g_{s\sigma}^R(\mathbf{k}, \omega) & g_{s\sigma}^K(\mathbf{k}, \omega) \end{pmatrix} \begin{pmatrix} d_{\sigma}^{cl} \\ d_{\sigma}^q \end{pmatrix} \right]. \end{aligned} \quad (\text{S92})$$

By defining the energy shift induced by the reservoirs

$$R_{\sigma}(\omega) = 2 \sum_{\mathbf{k}} |t_{\mathbf{k}}|^2 \text{Re} \left[g_{L\sigma}^R(\mathbf{k}, \omega) \right] = 2 \sum_{\mathbf{k}} |t_{\mathbf{k}}|^2 \text{Re} \left[g_{R\sigma}^R(\mathbf{k}, \omega) \right], \quad (\text{S93})$$

$$\Gamma_{\sigma}(\omega) = -2 \sum_{\mathbf{k}} |t_{\mathbf{k}}|^2 \text{Im} \left[g_{L\sigma}^R(\mathbf{k}, \omega) \right] = -2 \sum_{\mathbf{k}} |t_{\mathbf{k}}|^2 \text{Im} \left[g_{R\sigma}^R(\mathbf{k}, \omega) \right], \quad (\text{S94})$$

it follows that unperturbed Green's functions are given by

$$g_{11\sigma}^C(\tau, \tau') = -i \left\langle T_C \left[d_{0\sigma}(\tau) d_{0\sigma}^{\dagger}(\tau') \right] \right\rangle_0 \quad (\text{S95})$$

$$g_{d\sigma}^{R/A}(\omega) = \frac{1}{[\omega - \epsilon_0 - R_{\sigma}(\omega)] \pm i\Gamma_{\sigma}(\omega)}, \quad \left[g_{11\sigma}^{-1}(\omega) \right]^{R/A} = \omega - \epsilon_0 - R_{\sigma}(\omega) \pm i\Gamma_{\sigma}(\omega), \quad (\text{S96})$$

$$g_{11\sigma}^K(\omega) = \frac{-2i\Gamma_{\sigma}(\omega)(1 + \zeta n_{L\sigma}(\omega) + \zeta n_{R\sigma}(\omega))}{[\omega - \epsilon_0 - R_{\sigma}(\omega)]^2 + [\Gamma_{\sigma}(\omega)]^2}, \quad \left[g_{11\sigma}^{-1}(\omega) \right]^K = 2i\Gamma_{\sigma}(\omega)(1 + \zeta n_{L\sigma}(\omega) + \zeta n_{R\sigma}(\omega)), \quad (\text{S97})$$

where the distribution function $n_{s\sigma}(\omega)$ is

$$n_{s\sigma}(\omega) = \frac{1}{e^{(\omega - \Delta\mu_{s\sigma})/T_s} - \zeta}, \quad (\text{S98})$$

with $\mu = \sum_{s\sigma} \mu_{s\sigma}/4$ and $\Delta\mu_{s\sigma} = \mu_{s\sigma} - \mu$.

We next examine effects of V_{η} . In contrast to the dephasing model, the present setup does not allow the cancellation of complex diagrams, including crossing diagrams and bath renormalization diagrams. Therefore, we focus on the

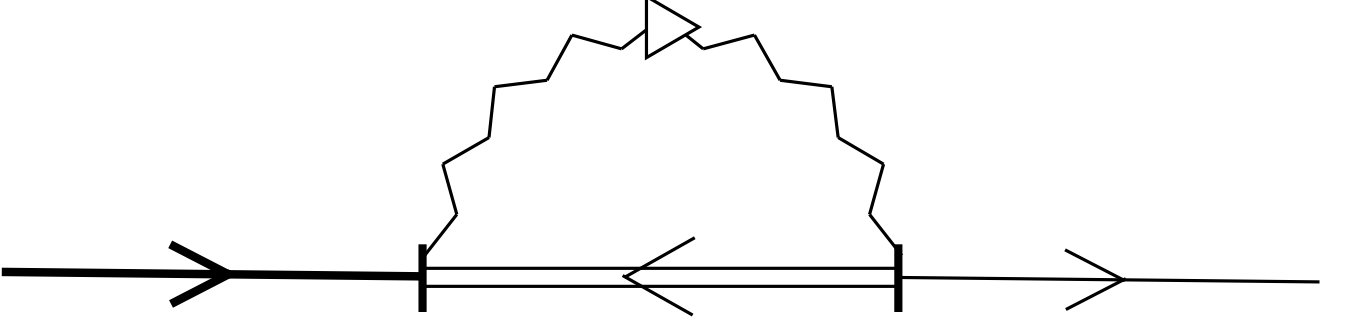


FIG. S6. SCBA diagram for two-particle loss.

weak-coupling regime, where dissipation can be treated perturbatively. Furthermore, to maintain consistency with the Lindblad dynamics, diagrams associated with bath renormalization must be excluded. To this end, we adopt the SCBA, which fulfills these conditions. Under this approximation, the contour-ordered Green's function satisfies

$$G_{11\sigma}^C(\tau, \tau') = g_{11\sigma}^C(\tau, \tau') + \int_C d\tau_1 \int_C d\tau_2 g_{11\sigma}^C(\tau, \tau_1) \Sigma_\sigma^C(\tau_1, \tau_2) G_{11\sigma}^C(\tau_2, \tau'), \quad (\text{S99})$$

where

$$\Sigma_\sigma^C(\tau, \tau') = i\zeta g_\eta^C(\tau, \tau') G_{11\bar{\sigma}}^C(\tau', \tau), \quad (\text{S100})$$

with the noise Green's functions

$$g_\eta^C(\tau, \tau') = -i \left\langle T_C [\eta(\tau) \eta^\dagger(\tau')] \right\rangle, \quad (\text{S101})$$

$$g_\eta^{R/A}(\tau, \tau') = \mp \frac{i}{2} \gamma \delta(\tau - \tau'), \quad (\text{S102})$$

$$g_\eta^K(\tau, \tau') = -i\gamma \delta(\tau - \tau') = g_\eta^>(\tau, \tau') = 2g_\eta^T(\tau, \tau') = 2g_\eta^{\bar{T}}(\tau, \tau'), \quad (\text{S103})$$

$$g_\eta^<(\tau, \tau') = 0. \quad (\text{S104})$$

The Langreth rules of the function $C^C(\tau, \tau') = A^C(\tau, \tau') B^C(\tau', \tau)$

$$C^R(\tau, \tau') = A^R(\tau, \tau') B^<(\tau', \tau) + A^<(\tau, \tau') B^A(\tau', \tau), \quad (\text{S105})$$

$$C^A(\tau, \tau') = A^<(\tau, \tau') B^R(\tau', \tau) + A^A(\tau, \tau') B^<(\tau', \tau), \quad (\text{S106})$$

$$C^K(\tau, \tau') = A^K(\tau, \tau') B^<(\tau', \tau) + A^<(\tau, \tau') (B^R(\tau', \tau) - B^A(\tau', \tau)), \quad (\text{S107})$$

and $g_\eta^<(\tau, \tau') = 0$ lead to

$$\Sigma_\sigma^{R/A/K}(\tau, \tau') = g_\eta^{R/A/K}(\tau, \tau') n_{0\bar{\sigma}}, \quad (\text{S108})$$

where

$$n_{0\sigma} = \frac{1}{-i\zeta} G_{11\sigma}^<(\tau, \tau) = \frac{1}{-i\zeta} \int_{-\infty}^{\infty} \frac{d\omega}{2\pi} G_{11\sigma}^<(\omega). \quad (\text{S109})$$

Each component of the Green's function is given by

$$G_{11\sigma}^{R/A}(\omega) = \frac{1}{[g_{d\sigma}^{-1}(\omega)]^{R/A} - \Sigma_\sigma^{R/A}(\omega)} = \frac{1}{\omega - \epsilon - R_\sigma(\omega) \pm i[\Gamma_\sigma(\omega) + \frac{\gamma}{2} n_{0\bar{\sigma}}]}, \quad (\text{S110})$$

$$G_{11\sigma}^K(\omega) = -G_{11\sigma}^R(\omega) \left([g_{d\sigma}^{-1}(\omega)]^K - \Sigma_\sigma^K(\omega) \right) G_{11\sigma}^A(\omega) = \frac{-2i(\Gamma_\sigma(\omega) + \frac{\gamma}{2} n_{d\bar{\sigma}}) - 2i\zeta \Gamma_\sigma(\omega)(n_{L\sigma}(\omega) + n_{R\sigma}(\omega))}{[\omega - \epsilon - R_\sigma(\omega)]^2 + [\Gamma_\sigma(\omega) + \frac{\gamma}{2} n_{0\bar{\sigma}}]^2}, \quad (\text{S111})$$

$$G_{11\sigma}^<(\omega) = \frac{-i\zeta \Gamma_\sigma(\omega)(n_{L\sigma}(\omega) + n_{R\sigma}(\omega))}{[\omega - \epsilon - R_\sigma(\omega)]^2 + [\Gamma_\sigma(\omega) + \frac{\gamma}{2} n_{0\bar{\sigma}}]^2}, \quad (\text{S112})$$

with the self-consistent integral equation

$$n_{0\sigma} = \int_{-\infty}^{\infty} \frac{d\omega}{2\pi} \frac{\Gamma_{\sigma}(\omega)(n_{L\sigma}(\omega) + n_{R\sigma}(\omega))}{[\omega - \epsilon - R_{\sigma}(\omega)]^2 + [\Gamma_{\sigma}(\omega) + \frac{\gamma}{2}n_{0\bar{\sigma}}]^2}. \quad (\text{S113})$$

The imaginary part of the reservoir's Green's function is proportional to a delta function

$$g_{s\sigma}^{R/A}(\mathbf{k}, \omega) = \frac{1}{(\omega - \Delta\mu_{s\sigma}) - (\epsilon_{\mathbf{k}} - \mu_{s\sigma}) \pm i0^+} = \mathcal{P} \left(\frac{1}{\omega + \mu - \epsilon_{\mathbf{k}}} \right) \mp i\pi\delta(\omega + \mu - \epsilon_{\mathbf{k}}), \quad (\text{S114})$$

$$g_{s\sigma}^K(\mathbf{k}, \omega) = -2\pi i\delta(\omega + \mu - \epsilon_{\mathbf{k}})(1 + 2\zeta n_{s\sigma}(\omega)), \quad (\text{S115})$$

leading to

$$\epsilon_{\mathbf{k}} \text{Im} [g_{s\sigma}^{R/A/K}(\mathbf{k}, \omega)] = (\omega + \mu) \text{Im} [g_{s\sigma}^{R/A/K}(\mathbf{k}, \omega)]. \quad (\text{S116})$$

Then, we obtain

$$\langle I_{s\sigma} \rangle = \int \frac{d\omega}{2\pi} [\mathcal{T}_{\sigma}(\omega)(2n_{s\sigma}(\omega) - n_{L\sigma}(\omega) - n_{R\sigma}(\omega)) + \mathcal{L}_{\sigma}(\omega)n_{s\sigma}(\omega)], \quad (\text{S117})$$

$$\langle I_{E,s\sigma} \rangle = \int \frac{d\omega}{2\pi} (\omega + \mu) [\mathcal{T}_{\sigma}(\omega)(2n_{s\sigma}(\omega) - n_{L\sigma}(\omega) - n_{R\sigma}(\omega)) + \mathcal{L}_{\sigma}(\omega)n_{s\sigma}(\omega)], \quad (\text{S118})$$

where $\mathcal{T}_{\sigma}(\omega)$ and $\mathcal{L}_{\sigma}(\omega)$ respectively represent the transmittance and loss probability defined as

$$\mathcal{T}_{\sigma}(\omega) = \frac{[\Gamma_{\sigma}(\omega)]^2}{[\omega - \epsilon - R_{\sigma}(\omega)]^2 + [\Gamma_{\sigma}(\omega) + \frac{\gamma}{2}n_{0\bar{\sigma}}]^2}, \quad (\text{S119})$$

$$\mathcal{L}_{\sigma}(\omega) = \frac{\Gamma_{\sigma}(\omega)\gamma n_{0\bar{\sigma}}}{[\omega - \epsilon - R_{\sigma}(\omega)]^2 + [\Gamma_{\sigma}(\omega) + \frac{\gamma}{2}n_{0\bar{\sigma}}]^2}. \quad (\text{S120})$$

The particle and energy currents are given by

$$I = \frac{1}{2} \sum_{\sigma} \left(\langle I_{L\sigma} \rangle - \langle I_{R\sigma} \rangle \right) = \sum_{\sigma} \int \frac{d\omega}{2\pi} \left[\mathcal{T}_{\sigma}(\omega) + \frac{\mathcal{L}_{\sigma}(\omega)}{2} \right] [n_{L\sigma}(\omega) - n_{R\sigma}(\omega)], \quad (\text{S121})$$

$$I_E = \frac{1}{2} \sum_{\sigma} \left(\langle I_{E,L\sigma} \rangle - \langle I_{E,R\sigma} \rangle \right) = \sum_{\sigma} \int \frac{d\omega}{2\pi} (\omega + \mu) \left[\mathcal{T}_{\sigma}(\omega) + \frac{\mathcal{L}_{\sigma}(\omega)}{2} \right] [n_{L\sigma}(\omega) - n_{R\sigma}(\omega)]. \quad (\text{S122})$$

In addition, the particle loss is obtained by

$$-\dot{N} = \sum_{\sigma} \left(\langle I_{L\sigma} \rangle + \langle I_{R\sigma} \rangle \right) = \sum_{\sigma} \int \frac{d\omega}{2\pi} \mathcal{L}_{\sigma}(\omega) [n_{L\sigma}(\omega) + n_{R\sigma}(\omega)] = \gamma \sum_{\sigma} n_{0\sigma} n_{0\bar{\sigma}} = 2\gamma n_{0\uparrow} n_{0\downarrow}. \quad (\text{S123})$$

VII. TWO-PARTICLE LOSS: MULTI-SITE CASE

In this section, we investigate the multi-site Hamiltonian

$$H = \sum_{s=L,R} \sum_{\sigma=\uparrow,\downarrow} H_{s\sigma} + H_T + \sum_{\alpha=0,\pm} H_{1D}^{\alpha}, \quad (\text{S124})$$

where

$$H_{s\sigma} = \sum_{\mathbf{k}} (\epsilon_{\mathbf{k}} - \mu_{s\sigma}) \psi_{s\mathbf{k}\sigma}^{\dagger} \psi_{s\mathbf{k}\sigma}, \quad (\text{S125})$$

$$H_T = - \sum_{s\mathbf{k}\sigma} \left(t_{\mathbf{k}} \psi_{s\mathbf{k}\sigma}^{\dagger} d_{0\sigma} + t_{\mathbf{k}}^* d_{0\sigma}^{\dagger} \psi_{s\mathbf{k}\sigma} \right), \quad (\text{S126})$$

$$H_{1D}^0 = \sum_{\sigma} \sum_{i=-N}^N \epsilon_i d_{i\sigma}^{\dagger} d_{i\sigma}, \quad (\text{S127})$$

$$H_{1D}^{\pm} = - \sum_{\sigma} \sum_{i=1}^N t_{\pm i} \left(d_{\pm i\sigma}^{\dagger} d_{\pm(i-1)\sigma} + d_{\pm(i-1)\sigma}^{\dagger} d_{\pm i\sigma} \right). \quad (\text{S128})$$

We introduce a two-particle loss in a quantum dot by the noise field

$$V_\eta = d_{0\uparrow}^\dagger d_{0\downarrow}^\dagger \eta + \eta^\dagger d_{0\downarrow} d_{0\uparrow}. \quad (\text{S129})$$

By employing the sane method as single-site case, we obtain

$$G_{dL(R)\sigma}^K(\mathbf{k}, \tau, \tau') = -i \left\langle \left[d_{-N(N)\sigma}(\tau), \psi_{\mathbf{k}L(R)\sigma}^\dagger(\tau) \right]_\zeta \right\rangle \quad (\text{S130})$$

$$= -t_{\mathbf{k}}^* \int_{-\infty}^{\infty} d\tau'' \left[G_{11(MM)\sigma}^R(\tau, \tau'') g_{L(R)\sigma}^K(\mathbf{k}, \tau'', \tau') + G_{11(MM)\sigma}^K(\tau, \tau'') g_{L(R)\sigma}^A(\mathbf{k}, \tau'', \tau') \right], \quad (\text{S131})$$

$$\begin{aligned} \langle I_{L(R)\sigma} \rangle &= \zeta \sum_{\mathbf{k}} \text{Re} \left[t_{\mathbf{k}} G_{dL(R)\sigma}^K(\mathbf{k}, \tau, \tau) \right] \\ &= -\zeta \int d\tau' \sum_{\mathbf{k}} |t_{\mathbf{k}}|^2 \text{Re} \left[G_{11(MM)\sigma}^R(\tau, \tau') g_{L(R)\sigma}^K(\mathbf{k}, \tau', \tau) + G_{11(MM)\sigma}^K(\tau, \tau') g_{L(R)\sigma}^A(\mathbf{k}, \tau', \tau) \right], \end{aligned} \quad (\text{S132})$$

$$\begin{aligned} \langle I_{E,L(R)\sigma} \rangle &= \zeta \sum_{\mathbf{k}} \epsilon_{\mathbf{k}} \text{Re} \left[t_{\mathbf{k}} G_{dL(R)\sigma}^K(\mathbf{k}, \tau, \tau) \right] \\ &= -\zeta \int d\tau' \sum_{\mathbf{k}} \epsilon_{\mathbf{k}} |t_{\mathbf{k}}|^2 \text{Re} \left[G_{11(MM)\sigma}^R(\tau, \tau') g_{L(R)\sigma}^K(\mathbf{k}, \tau', \tau) + G_{11(MM)\sigma}^K(\tau, \tau') g_{L(R)\sigma}^A(\mathbf{k}, \tau', \tau) \right], \end{aligned} \quad (\text{S133})$$

where

$$G_{ij\sigma}^C(\tau, \tau') = -i \left\langle T_C \left[d_{(i-N-1)\sigma}(\tau) d_{(j-N-1)\sigma}^\dagger(\tau') \right] \right\rangle. \quad (\text{S134})$$

The retarded and advanced components of the matrix of the Green's function

$$\mathbf{G}_{d\sigma}^C = \begin{pmatrix} G_{11\sigma}^C & G_{12\sigma}^C & \cdots & G_{1M\sigma}^C \\ G_{21\sigma}^C & G_{22\sigma}^C & \cdots & G_{2M\sigma}^C \\ \vdots & \vdots & \ddots & \vdots \\ G_{M1\sigma}^C & G_{M2\sigma}^C & \cdots & G_{MM\sigma}^C \end{pmatrix}, \quad (\text{S135})$$

is given by

$$\left[\mathbf{G}_{d\sigma}^{-1}(\omega) \right]^{R/A} = \left[\mathbf{g}_{d\sigma}^{-1}(\omega) \right]^{R/A} + \Sigma_{d\sigma}^{R/A}, \quad (\text{S136})$$

where

$$\left[\mathbf{g}_{d\sigma}^{-1}(\omega) \right]^{R/A} = \begin{pmatrix} \omega - \epsilon_{-N} \pm i0^+ & 0 & \cdots & 0 & \cdots & 0 \\ 0 & \omega - \epsilon_{-N-1} \pm i0^+ & \cdots & 0 & \cdots & 0 \\ \vdots & \vdots & \ddots & \vdots & \ddots & \vdots \\ 0 & 0 & \cdots & \omega - \epsilon_0 \pm i0^+ & \cdots & 0 \\ \vdots & \vdots & \ddots & \vdots & \ddots & \vdots \\ 0 & 0 & \cdots & 0 & \cdots & \omega - \epsilon_N \pm i0^+ \end{pmatrix}, \quad (\text{S137})$$

$$\Sigma_{d\sigma}^{R/A}(\omega) = \begin{pmatrix} \frac{R_\sigma(\omega) \mp i\Gamma_\sigma(\omega)}{2} & -t_{-N} & \cdots & 0 & \cdots & \cdots & 0 \\ -t_{-N} & 0 & \cdots & \cdots & \cdots & \cdots & 0 \\ \vdots & \vdots & \ddots & -t_{-1} & \ddots & \cdots & \vdots \\ 0 & \cdots & -t_{-1} & \mp i\frac{\gamma}{2} n_{0\bar{\sigma}} & -t_1 & \cdots & 0 \\ \vdots & \vdots & \ddots & -t_1 & \ddots & \ddots & \vdots \\ \vdots & \vdots & \ddots & \vdots & \ddots & \ddots & -t_N \\ 0 & 0 & \cdots & \cdots & \cdots & -t_N & \frac{R_\sigma(\omega) \mp i\Gamma_\sigma(\omega)}{2} \end{pmatrix}. \quad (\text{S138})$$

The inverse of a tridiagonal matrix

$$T = \begin{pmatrix} a_1 & b_1 & \cdots & 0 \\ c_1 & a_2 & \ddots & \vdots \\ \vdots & \ddots & \ddots & b_{L-1} \\ 0 & \cdots & c_{L-1} & a_L \end{pmatrix}, \quad (\text{S139})$$

is obtained by

$$[T^{-1}]_{ij} = \begin{cases} (-1)^{i+j} b_i \cdots b_{j-1} \theta_{i-1} \phi_{j+1} / \theta_L & (i < j) \\ \theta_{i-1} \phi_{j+1} / \theta_L & (i = j) \\ (-1)^{i+j} c_j \cdots c_{i-1} \theta_{j-1} \phi_{i+1} / \theta_L & (i > j) \end{cases}, \quad (\text{S140})$$

where

$$\begin{aligned} \theta_i &= a_i \theta_{i-1} - b_{i-1} c_{i-1} \theta_{i-2} \quad (i = 2, 3, \dots, L), \quad \theta_0 = 1, \quad \theta_1 = a_1, \\ \phi_i &= a_i \phi_{i+1} - b_i c_i \phi_{i+2} \quad (i = 1, 2, \dots, L-1), \quad \phi_L = a_L, \quad \phi_{L+1} = 1. \end{aligned}$$

The Keldysh component of the matrix of the Green's function is given by

$$\mathbf{G}_{d\sigma}^K(\omega) = \mathbf{G}_{d\sigma}^R(\omega) \mathbf{\Sigma}_{d\sigma}^K(\omega) \mathbf{G}_{d\sigma}^A(\omega), \quad (\text{S141})$$

where

$$\mathbf{\Sigma}_{d\sigma}^K(\omega) = \begin{pmatrix} -i\Gamma_\sigma(\omega)[1 + 2\zeta n_{L\sigma}(\omega)] & & & & \\ & \ddots & & & \\ & & -i\gamma n_{0\bar{\sigma}} & & \\ & & & \ddots & \\ & & & & -i\Gamma_\sigma(\omega)[1 + 2\zeta n_{R\sigma}(\omega)] \end{pmatrix}.$$

The (ij) elements is obtained by

$$\begin{aligned} G_{ij\sigma}^K(\omega) &= G_{i1\sigma}^R(\omega) \left\{ -i\Gamma_\sigma(\omega)[1 + 2\zeta n_{L\sigma}(\omega)] \right\} G_{1j\sigma}^A(\omega) \\ &+ G_{i\frac{M+1}{2}\sigma}^R(\omega) \left\{ -i\gamma n_{0\bar{\sigma}} \right\} G_{\frac{M+1}{2}j\sigma}^A(\omega) \\ &+ G_{iM\sigma}^R(\omega) \left\{ -i\Gamma_\sigma(\omega)[1 + 2\zeta n_{R\sigma}(\omega)] \right\} G_{Mj\sigma}^A(\omega). \end{aligned}$$

In particular, the $(ij) = (11)$ element is

$$G_{11\sigma}^K(\omega) = \left\{ -i\Gamma_\sigma(\omega)[1 + 2\zeta n_{L\sigma}(\omega)] \right\} \left| G_{11\sigma}^R(\omega) \right|^2 \quad (\text{S142})$$

$$+ \left\{ -i\gamma n_{0\bar{\sigma}} \right\} \left| G_{1\frac{M+1}{2}\sigma}^R(\omega) \right|^2 \quad (\text{S143})$$

$$+ \left\{ -i\Gamma_\sigma(\omega)[1 + 2\zeta n_{R\sigma}(\omega)] \right\} \left| G_{1M\sigma}^R(\omega) \right|^2, \quad (\text{S144})$$

and the $(ij) = (MM)$ element is

$$G_{MM\sigma}^K(\omega) = \left\{ -i\Gamma_\sigma(\omega)[1 + 2\zeta n_{L\sigma}(\omega)] \right\} \left| G_{M1\sigma}^R(\omega) \right|^2 \quad (\text{S145})$$

$$+ \left\{ -i\gamma n_{0\bar{\sigma}} \right\} \left| G_{M\frac{M+1}{2}\sigma}^R(\omega) \right|^2 \quad (\text{S146})$$

$$+ \left\{ -i\Gamma_\sigma(\omega)[1 + 2\zeta n_{R\sigma}(\omega)] \right\} \left| G_{MM\sigma}^R(\omega) \right|^2, \quad (\text{S147})$$

with the property of the Green's function $G^A = [G^R]^\dagger$. The inverse matrix inherits the following symmetries possessed by the original matrix

$$A^T = A \quad \Rightarrow \quad (A^{-1})^T = A^{-1}, \quad (\text{S148})$$

$$A_{ij} = A_{M-j+1, M-i+1} \quad \Rightarrow \quad (A^{-1})_{ij} = (A^{-1})_{(M-j+1)(M-i+1)}, \quad (\text{S149})$$

because

$$I = I^T = (AA^{-1})^T = (A^{-1})^T A^T = (A^{-1})^T A, \quad (\text{S150})$$

$$\delta_{ij} = \sum_{k=1}^M A_{ik} (A^{-1})_{kj} = \sum_{k=1}^M A_{(M-k+1)(M-i+1)} (A^{-1})_{kj} = \sum_{l=1}^M (A^{-1})_{lj} A_{(M-l+1)(M-i+1)} \quad (\text{S151})$$

$$= \delta_{(M-j+1)(M-i+1)} = \sum_{k=1}^M (A^{-1})_{(M-j+1)k} A_{k(M-i+1)} = \sum_{l=1}^M (A^{-1})_{(M-j+1)(M-l+1)} A_{(M-l+1)(M-i+1)}. \quad (\text{S152})$$

By using the above symmetries

$$G_{11\sigma}^R(\omega) = G_{MM\sigma}^R(\omega), \quad G_{1\frac{M+1}{2}\sigma}^R(\omega) = G_{\frac{M+1}{2}1\sigma}^R(\omega) = G_{M\frac{M+1}{2}\sigma}^R(\omega) = G_{\frac{M+1}{2}M\sigma}^R(\omega), \quad (\text{S153})$$

we obtain

$$\begin{aligned} \langle I_{L(R)\sigma} \rangle &= -\zeta \int \frac{d\omega}{2\pi} \Gamma_\sigma(\omega) \text{Im} \left[G_{11\sigma}^R(\omega) \right] [1 + 2\zeta n_{L(R)\sigma}(\omega)] \\ &\quad - \zeta \int \frac{d\omega}{2\pi} \Gamma_\sigma(\omega) \frac{\Gamma_\sigma(\omega) \left([1 + 2\zeta n_{L(R)\sigma}(\omega)] \left| G_{11\sigma}^R(\omega) \right|^2 + [1 + 2\zeta n_{R(L)\sigma}(\omega)] \left| G_{1M\sigma}^R(\omega) \right|^2 \right)}{2} \\ &\quad - \zeta \int \frac{d\omega}{2\pi} \Gamma_\sigma(\omega) \frac{\gamma n_{0\bar{\sigma}} \left| G_{1\frac{M+1}{2}\sigma}^R(\omega) \right|^2}{2}, \end{aligned} \quad (\text{S154})$$

$$\begin{aligned} \langle I_{E,L(R)\sigma} \rangle &= -\zeta \int \frac{d\omega}{2\pi} (\omega + \mu) \Gamma_\sigma(\omega) \text{Im} \left[G_{11\sigma}^R(\omega) \right] [1 + 2\zeta n_{L(R)\sigma}(\omega)] \\ &\quad - \zeta \int \frac{d\omega}{2\pi} (\omega + \mu) \Gamma_\sigma(\omega) \frac{\Gamma_\sigma(\omega) \left([1 + 2\zeta n_{L(R)\sigma}(\omega)] \left| G_{11\sigma}^R(\omega) \right|^2 + [1 + 2\zeta n_{R(L)\sigma}(\omega)] \left| G_{1M\sigma}^R(\omega) \right|^2 \right)}{2} \\ &\quad - \zeta \int \frac{d\omega}{2\pi} (\omega + \mu) \Gamma_\sigma(\omega) \frac{\gamma n_{0\bar{\sigma}} \left| G_{1\frac{M+1}{2}\sigma}^R(\omega) \right|^2}{2}. \end{aligned} \quad (\text{S155})$$

The particle and energy currents, and particle loss are given by

$$I = \sum_\sigma \int \frac{d\omega}{2\pi} \Gamma_\sigma(\omega) \left[-\text{Im} \left[G_{11\sigma}^R(\omega) \right] - \frac{\Gamma_\sigma(\omega) \left(\left| G_{11\sigma}^R(\omega) \right|^2 - \left| G_{ML\sigma}^R(\omega) \right|^2 \right)}{2} \right] [n_{L\sigma}(\omega) - n_{R\sigma}(\omega)], \quad (\text{S156})$$

$$I_E = \sum_\sigma \int \frac{d\omega}{2\pi} (\omega + \mu) \Gamma_\sigma(\omega) \left[-\text{Im} \left[G_{11\sigma}^R(\omega) \right] - \frac{\Gamma_\sigma(\omega) \left(\left| G_{11\sigma}^R(\omega) \right|^2 - \left| G_{ML\sigma}^R(\omega) \right|^2 \right)}{2} \right] [n_{L\sigma}(\omega) - n_{R\sigma}(\omega)], \quad (\text{S157})$$

$$\begin{aligned} -\dot{N} &= -\zeta \sum_\sigma \int \frac{d\omega}{2\pi} \Gamma_\sigma(\omega) \left[2 \text{Im} \left[G_{11\sigma}^R(\omega) \right] + \Gamma_\sigma(\omega) \left(\left| G_{11\sigma}^R(\omega) \right|^2 + \left| G_{1M\sigma}^R(\omega) \right|^2 \right) + \gamma n_{0\bar{\sigma}} \left| G_{1\frac{M+1}{2}\sigma}^R(\omega) \right|^2 \right] \\ &\quad - \sum_\sigma \int \frac{d\omega}{2\pi} \Gamma_\sigma(\omega) \left[2 \text{Im} \left[G_{11\sigma}^R(\omega) \right] + \Gamma_\sigma(\omega) \left(\left| G_{11\sigma}^R(\omega) \right|^2 + \left| G_{1M\sigma}^R(\omega) \right|^2 \right) \right] [n_{L\sigma}(\omega) + n_{R\sigma}(\omega)]. \end{aligned} \quad (\text{S158})$$

The identity

$$\mathbf{G}_{d\sigma}^R - \mathbf{G}_{d\sigma}^A = \mathbf{G}_{d\sigma}^R \left[\left(\mathbf{G}_{d\sigma}^A \right)^{-1} - \left(\mathbf{G}_{d\sigma}^R \right)^{-1} \right] \mathbf{G}_{d\sigma}^A = \mathbf{G}_{d\sigma}^R \left[\boldsymbol{\Sigma}_{d\sigma}^R - \boldsymbol{\Sigma}_{d\sigma}^A \right] \mathbf{G}_{d\sigma}^A, \quad (\text{S159})$$

leads to

$$\begin{aligned} &2i \text{Im} \left[G_{11\sigma}^R(\omega) \right] \\ &= G_{11\sigma}^R(\omega) - G_{11\sigma}^A(\omega) \\ &= G_{11\sigma}^R(\omega) \left(-i\Gamma(\omega) \right) G_{11\sigma}^A(\omega) + G_{1\frac{M+1}{2}\sigma}^R(\omega) \left(-i\gamma n_{0\bar{\sigma}} \right) G_{\frac{M+1}{2}1\sigma}^A(\omega) + G_{1M\sigma}^R(\omega) \left(-i\Gamma(\omega) \right) G_{1M\sigma}^A(\omega) \\ &= -i \left[\Gamma(\omega) \left\{ \left| G_{11\sigma}^R(\omega) \right|^2 + \left| G_{1M\sigma}^R(\omega) \right|^2 \right\} + \gamma n_{0\bar{\sigma}} \left| G_{1\frac{M+1}{2}\sigma}^R(\omega) \right|^2 \right], \end{aligned} \quad (\text{S160})$$

Thus, we obtain

$$2 \operatorname{Im} \left[G_{11\sigma}^R(\omega) \right] + \Gamma(\omega) \left(\left| G_{11\sigma}^R(\omega) \right|^2 + \left| G_{1M\sigma}^R(\omega) \right|^2 \right) + \gamma n_{0\bar{\sigma}} \left| G_{1\frac{M+1}{2}\sigma}^R(\omega) \right|^2 = 0. \quad (\text{S161})$$

In total, we reach the following expressions:

$$I = \sum_{\sigma} \int \frac{d\omega}{2\pi} \left[\mathcal{T}_{\sigma}^M(\omega) + \frac{\mathcal{L}_{\sigma}^M(\omega)}{2} \right] [n_{L\sigma}(\omega) - n_{R\sigma}(\omega)], \quad (\text{S162})$$

$$I_E = \sum_{\sigma} \int \frac{d\omega}{2\pi} (\omega + \bar{\mu}) \left[\mathcal{T}_{\sigma}^M(\omega) + \frac{\mathcal{L}_{\sigma}^M(\omega)}{2} \right] [n_{L\sigma}(\omega) - n_{R\sigma}(\omega)], \quad (\text{S163})$$

$$-\dot{N} = \sum_{\sigma} \int \frac{d\omega}{2\pi} \mathcal{L}_{\sigma}^M(\omega) [n_{L\sigma}(\omega) + n_{R\sigma}(\omega)], \quad (\text{S164})$$

where

$$\mathcal{T}_{\sigma}^M(\omega) = \left[\Gamma_{\sigma}(\omega) \right]^2 \left| G_{1M\sigma}^R(\omega) \right|^2, \quad \mathcal{L}_{\sigma}^M(\omega) = \left[\Gamma_{\sigma}(\omega) \gamma n_{0\bar{\sigma}} \right] \left| G_{1\frac{M+1}{2}\sigma}^R(\omega) \right|^2. \quad (\text{S165})$$

We can also obtain the convenient expression of the particle loss. Since the lesser Green's function possesses the following structure:

$$\begin{aligned} \mathbf{G}_{d\sigma}^<(\omega) &= \frac{\mathbf{G}_{d\sigma}^K(\omega) - (\mathbf{G}_{d\sigma}^R(\omega) - \mathbf{G}_{d\sigma}^A(\omega))}{2} \\ &= \mathbf{G}_{d\sigma}^R(\omega) \frac{\boldsymbol{\Sigma}_{d\sigma}^K(\omega) - (\boldsymbol{\Sigma}_{d\sigma}^R(\omega) - \boldsymbol{\Sigma}_{d\sigma}^A(\omega))}{2} \mathbf{G}_{d\sigma}^A(\omega) \\ &= -i\zeta \Gamma_{\sigma}(\omega) \mathbf{G}_{d\sigma}^R(\omega) \begin{pmatrix} n_{L\sigma}(\omega) & & \\ & \ddots & \\ & & n_{R\sigma}(\omega) \end{pmatrix} \mathbf{G}_{d\sigma}^A(\omega), \end{aligned} \quad (\text{S166})$$

we have

$$\begin{aligned} G_{\frac{M+1}{2}\frac{M+1}{2}\sigma}^<(\omega) &= -i\zeta \Gamma_{\sigma}(\omega) \left[\left| G_{\frac{M+1}{2}1}^R(\omega) \right|^2 n_{L\sigma}(\omega) + \left| G_{\frac{M+1}{2}M}^R(\omega) \right|^2 n_{R\sigma}(\omega) \right] \\ &= -i\zeta \Gamma_{\sigma}(\omega) \left| G_{1\frac{M+1}{2}}^R(\omega) \right|^2 [n_{L\sigma}(\omega) + n_{R\sigma}(\omega)]. \end{aligned} \quad (\text{S167})$$

By using the above equation, we obtain

$$n_{0\sigma} = \frac{1}{-i\zeta} \int \frac{d\omega}{2\pi} G_{\frac{M+1}{2}\frac{M+1}{2}\sigma}^<(\omega) = \int \frac{d\omega}{2\pi} \Gamma_{\sigma}(\omega) \left| G_{1\frac{M+1}{2}}^R(\omega) \right|^2 [n_{L\sigma}(\omega) + n_{R\sigma}(\omega)]. \quad (\text{S168})$$

The same expression in the single-site case is given by

$$-\dot{N} = 2\gamma n_{0\uparrow} n_{0\downarrow}. \quad (\text{S169})$$

-
- [1] H.-P. Breuer and F. Petruccione, *The theory of open quantum systems* (OUP Oxford, 2002).
 - [2] P. E. Dolgirev, J. Marino, D. Sels, and E. Demler, Non-gaussian correlations imprinted by local dephasing in fermionic wires, *Phys. Rev. B* **102**, 100301(R) (2020).
 - [3] T. Jin, J. a. S. Ferreira, M. Filippone, and T. Giamarchi, Exact description of quantum stochastic models as quantum resistors, *Phys. Rev. Res.* **4**, 013109 (2022).
 - [4] A. Kamenev, *Field theory of non-equilibrium systems* (Cambridge University Press, 2023).

Quantum Point Contact with Local Two-body Loss

Kensuke Kakimoto

Department of Electronic and Physical Systems, Waseda University, Tokyo 169-8555, Japan

Shun Uchino

*Department of Electronic and Physical Systems, Waseda University, Tokyo 169-8555, Japan and
Department of Materials Science, Waseda University, Tokyo 169-8555, Japan*

(Dated: June 10, 2025)

Motivated by recent advances in ultracold atomic gas experiments, we investigate a two-terminal mesoscopic system in which two-body loss occurs locally at the center of a one-dimensional chain. By means of the self-consistent Born approximation in the Keldysh formalism, we uncover mesoscopic current formulas that are experimentally relevant and applicable to the weak dissipation regime. Although these formulas are analogous to those for systems with one-body loss, it turns out that the channel transmittance and loss probability depend on the nonequilibrium occupation at the lossy site. We demonstrate that this occupation dependence leads to a weaker suppression of currents in the presence of two-body loss compared to one-body loss, in agreement with a recent experimental observation.

Introduction.—Open quantum systems provide a natural arena for exploring the interplay between coherent dynamics and dissipative processes [1, 2]. In contrast to isolated systems, where unitary evolution governs dynamics, coupling to an environment introduces decoherence and particle loss, fundamentally altering transport properties and steady-state behaviors [2, 3]. Recent advances have revealed that such dissipation can induce nontrivial quantum phenomena, including nonequilibrium quantum criticality [4, 5], many-body quantum Zeno effect [6–11], and unconventional renormalization-group flows in strongly correlated settings [12, 13].

The development of highly controllable platforms, particularly ultracold atomic gases, has enabled systematic investigation of engineered dissipation in many-body systems [14–16]. In these setups, particle losses realized via focused light fields and photo-association can be tuned with high precision, allowing experimental access to particle-loss processes [9, 17–26]. These capabilities have motivated a new class of transport experiments that probe the role of dissipation in mesoscopic conduction, with ultracold analogs of quantum point contacts (QPCs) serving as the core geometry [27, 28].

Of particular interest is the recent realization of a two-terminal QPC setup exhibiting localized loss in a one-dimensional (1D) channel. Previous theoretical and experimental efforts have primarily focused on one-body loss [29–37], where dissipation effects can be effectively captured with introduction of an additional reservoir in which injection into the channel is prohibited.

In contrast, local two-body loss exhibits fundamentally different characteristics from one-body loss, as it only occurs when two particles simultaneously occupy a spatially restricted region. This constraint renders two-body loss inherently a many-body effect, as explicitly captured by the nonequilibrium many-body formalism [16, 38]. This many-body nature suggests qualitatively distinct transport behavior due to the nonlinear feedback between occupation and loss. In particular, un-

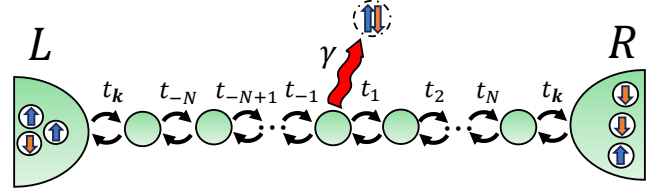


FIG. 1. Schematic of the mesoscopic transport setup: two normal reservoirs are connected via a 1D chain representing a QPC. The local two-body loss, with rate γ , occurs at the central site when the spin-up and spin-down particles are simultaneously present.

der nonequilibrium steady-state conditions driven chemical potential and temperature gradients, such dissipation may alter particle and energy currents in ways that elude straightforward extensions of the Landauer-Büttiker formalism [3, 39]. Despite its conceptual and experimental relevance, a theoretical framework for quantum transport incorporating two-body loss has remained largely unexplored.

In this Letter, we theoretically investigate two-terminal transport through a 1D chain with localized two-body loss, modeling a dissipative QPC. To this end, we develop the Keldysh Green’s function formalism combined with a noise-field representation of Lindblad dynamics [40–42]. By applying the self-consistent Born approximation (SCBA) [43] that is valid in a weak dissipative regime and is also consistent with the quantum master equation approach, we derive analytic expressions for mesoscopic particle and energy currents. We find that the effective loss rate becomes occupation-dependent, resulting in weaker current suppression compared to one-body loss. This result is in agreement with a recent experimental observation in ultracold atomic gases.

The model.—We consider a system where two normal macroscopic reservoirs are connected via a QPC (Fig. 1).

The corresponding Hamiltonian is given by

$$H = \sum_{s=L,R} \sum_{\sigma=\uparrow,\downarrow} H_{s\sigma} + H_T + \sum_{\alpha=0,\pm} H_{1D}^\alpha, \quad (1)$$

$$H_T = - \sum_{\mathbf{k},\sigma} t_{\mathbf{k}} \left(\psi_{L\mathbf{k}\sigma}^\dagger d_{-N\sigma} + \psi_{R\mathbf{k}\sigma}^\dagger d_{N\sigma} \right) + \text{H.c.}, \quad (2)$$

$$H_{1D}^\pm = - \sum_{\sigma} \sum_{i=1}^N t_{\pm i} \left(d_{\pm i\sigma}^\dagger d_{\pm(i-1)\sigma} + d_{\pm(i-1)\sigma}^\dagger d_{\pm i\sigma} \right). \quad (3)$$

The Hamiltonian of the left (right) reservoir with spin σ , $H_{L(R)\sigma} = \sum_{\mathbf{k}} (\epsilon_{\mathbf{k}} - \mu_{L(R)\sigma}) \psi_{L(R)\mathbf{k}\sigma}^\dagger \psi_{L(R)\mathbf{k}\sigma}$ is expressed with the kinetic energy $\epsilon_{\mathbf{k}} = \mathbf{k}^2/2m$, the chemical potential $\mu_{L(R)\sigma}$, and the field annihilation (creation) operator $\psi_{L(R)\mathbf{k}\sigma}$ ($\psi_{L(R)\mathbf{k}\sigma}^\dagger$). We model a QPC with the 1D chain, which is composed of the hopping term between different sites H_{1D}^\pm and the onsite energy term $H_{1D}^0 = \sum_{\sigma} \sum_{i=-N}^N \epsilon_i d_{i\sigma}^\dagger d_{i\sigma}$, with a potential of energy ϵ_i and annihilation (creation) operator in the 1D chain $d_{i\sigma}$ ($d_{i\sigma}^\dagger$). In addition, tunneling between reservoirs and 1D chain occurring at the edges of the 1D chain is expressed in H_T with the tunnel coupling strength $t_{\mathbf{k}}$.

We next consider two-body loss occurring at the central site of the 1D chain and treat dissipation within the Markovian Lindblad master equation [1]. We note that such a Markovian treatment is relevant to ultracold atomic gases [14] and has successfully been employed to interpret recent results on dissipative quantum transport [26, 35]. Typically, the open quantum dynamics is analyzed by following the non-unitary evolution of the density matrix, which involves both non-Hermitian and quantum jump terms in addition to the unitary dynamics. This treatment is in sharp contrast to the standard approaches in many-body physics such as quantum field theory. To enable a field-theoretic analysis of dissipation, we adopt the Hamiltonian formalism incorporating noise fields [40–42, 44, 45]. In this framework, two-body loss is captured by adding the term

$$V_\eta = d_{0\uparrow}^\dagger d_{0\downarrow}^\dagger \eta + \eta^\dagger d_{0\downarrow} d_{0\uparrow}, \quad (4)$$

which describes pair loss at the central site when spin-up and spin-down particles are simultaneously present. Provided that noise fields η and η^\dagger satisfy the following statistical properties:

$$\begin{aligned} \langle \eta(\tau) \eta^\dagger(\tau') \rangle_\eta &= \gamma \delta(\tau - \tau'), \\ \langle \eta^\dagger(\tau) \eta(\tau') \rangle_\eta &= \langle \eta(\tau) \eta(\tau') \rangle_\eta = 0, \end{aligned} \quad (5)$$

with the dissipation strength γ , resulting dynamics can reproduce those governed by the quantum master equation with Lindblad operator $d_{0\downarrow} d_{0\uparrow}$, which accounts for two-body loss, subject to certain considerations discussed below [46].

Based on the Hamiltonian comprised of two-terminal and noise field terms, the particle and energy currents can be expressed as $I = \sum_{\sigma} [-\dot{N}_{L\sigma} + \dot{N}_{R\sigma}]$ and $I_E = \sum_{\sigma} [-\dot{H}_{L\sigma} - \mu_{L\sigma} \dot{N}_{L\sigma} + \dot{H}_{R\sigma} + \mu_{R\sigma} \dot{N}_{R\sigma}]$, respectively. As in closed quantum many-body systems, these current expressions can be transformed into more convenient forms as follows: [34, 47]

$$\begin{aligned} \dot{N}_{L(R)\sigma} &= \zeta \int \frac{d\omega}{2\pi} \sum_{\mathbf{k}} |t_{\mathbf{k}}|^2 \text{Re} \left[G_{11(MM)\sigma}^R(\omega) g_{L(R)\sigma}^K(\mathbf{k}, \omega) \right] \\ &\quad + \zeta \int \frac{d\omega}{2\pi} \sum_{\mathbf{k}} |t_{\mathbf{k}}|^2 \text{Re} \left[G_{11(MM)\sigma}^K(\omega) g_{L(R)\sigma}^A(\mathbf{k}, \omega) \right], \end{aligned} \quad (6)$$

$$\begin{aligned} \dot{H}_{L(R)\sigma} + \mu_{L(R)\sigma} \dot{N}_{L(R)\sigma} &= \zeta \int \frac{d\omega}{2\pi} \sum_{\mathbf{k}} \epsilon_{\mathbf{k}} |t_{\mathbf{k}}|^2 \text{Re} \left[G_{11(MM)\sigma}^R(\omega) g_{L(R)\sigma}^K(\mathbf{k}, \omega) \right] \\ &\quad + \zeta \int \frac{d\omega}{2\pi} \sum_{\mathbf{k}} \epsilon_{\mathbf{k}} |t_{\mathbf{k}}|^2 \text{Re} \left[G_{11(MM)\sigma}^K(\omega) g_{L(R)\sigma}^A(\mathbf{k}, \omega) \right], \end{aligned} \quad (7)$$

where $\zeta = +1(-1)$ for bosons (fermions) and $M = 2N+1$ is the number of the site. Here, $g_{L(R)\sigma}^{K/A}$ is the unperturbed Keldysh/advanced Green's function of the left (right) reservoir with spin σ and is easily evaluated in equilibrium in which fluctuation-dissipation theorem holds [38]. In contrast, $G_{ij\sigma}^{K/A}$ is full Keldysh/retarded Green's function of the 1D chain and is extracted from the corresponding contour-ordered Green's function $G_{ij\sigma}^C(\tau, \tau') = -i \langle T_C [d_{(i-N-1)\sigma}(\tau) d_{(j-N-1)\sigma}^\dagger(\tau')] \rangle$ with contour-ordering T_C [46].

Noise field formalism.—The evaluation of the particle and energy currents [Eqs. (6) and (7)] reduces to computing the full Green's functions $G_{11(MM)\sigma}^{K/R}$. Treating V_η as a perturbation, we employ the Feynman diagram technique to systematically evaluate these functions. Notably, the noise field formalism shares similarity with the treatment of disorder potentials [48] in that both involve statistical averaging. However, a complication in the present context arises from the temporal correlations imposed by Eq. (5). The Keldysh formalism then provides a natural framework to incorporate these correlation effects in a systematic manner.

When the Lindblad operator involves two field operators, as in the case of two-body loss and dephasing [1, 16], the system-environment coupling effectively behaves as a two-body interaction upon averaging over the noise field [42]. However, unlike genuine interactions, this coupling connects time arguments on the forward and backward branches of the Keldysh contour [16]. This branch mixing leads to qualitative differences from conventional two-body interactions [46].

In the dephasing model, where the Lindblad operator is $d^\dagger d$ and the associated noise operator is Hermitian, the SCBA yields exact results [41, 42]. This exactness arises from the symmetric contributions of all components of the contour-ordered Green's function for

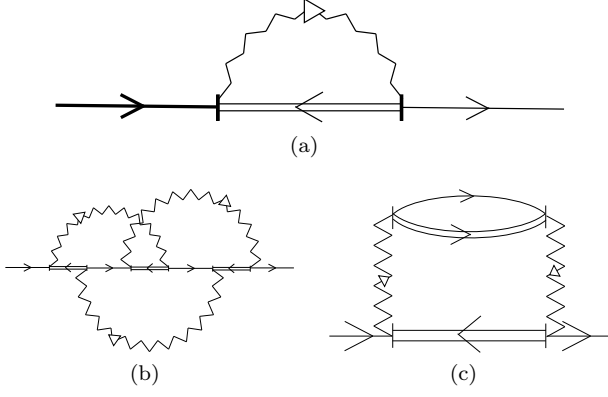


FIG. 2. (a) Feynman diagram corresponding to the SCBA. (b) Crossing diagram neglected in the SCBA. (c) Diagram to be discarded for consistency with the Lindblad master equation. The thin line represents the unperturbed Green's function of the particle with spin σ , g_σ^C , the thick line the full Green's function of the particle with spin σ , G_σ^C , the double line in Fig. 2(a) the full Green function of the particle with opposite spin $\bar{\sigma}$, $G_{\bar{\sigma}}^C$, the double line in Fig. 2(b) and 2(c) the unperturbed Green function of the particle with opposite spin $\bar{\sigma}$, $g_{\bar{\sigma}}^C$, and the wavy line the Green's function for the noise field, g_η^C .

the noise field g_η^C , which leads to the systematic cancellation of all higher-order Feynman diagrams beyond the SCBA [46].

We now turn to the case of two-body loss, where the Lindblad operator is $d_{0\downarrow}d_{0\uparrow}$. In contrast to the dephasing model, here the systematic cancellation of Feynman diagrams does not occur, preventing an exact evaluation via the Feynman diagram technique. We find that this complication arises because the noise averages specified in Eq. (5) lead to asymmetric contributions from the time components of the contour-ordered noise-field Green's functions [46].

To elucidate the essential differences in quantum transport with and without dissipation, we focus on a regime in which dissipation is amenable to a perturbative treatment. We point out that this weakly dissipative regime is relevant to the recent experiment in which local two-body loss is controlled via photo-association provided by an optical tweezer [26]. When it comes to this regime, it is reasonable to neglect multiple scattering by the noise fields. This leads to the SCBA, which accounts for processes where a spin- σ particle interacts with an opposite-spin particle at via noise fields (See Fig. 2(a)), while neglecting the crossing diagrams (such as Fig. 2(b)). The SCBA does not also contain a process in which spin-up and spin-down particles are transiently created as pairs by the noise field, propagate, and subsequently annihilate, as illustrated in Fig. 2(c). Physically, this diagram corresponds to an effective bath renormalization effect induced by the finite system. We point out that for consistency with the Lindblad equation, such a diagram must rather be discarded [46].

Single-site case—To clarify the essential role of two-body loss in two-terminal transport, we first consider the simplest case of a single-site system, $M = 1$.

To evaluate $G_{11\sigma}^{R/K}$ we harness the Dyson equation in the Keldysh formalism. Under the SCBA, the contour-ordered Green's function obeys

$$G_{11\sigma}^C = g_{11\sigma}^C + g_{11\sigma}^C \circ \Sigma_{11\sigma}^C \circ G_{11\sigma}^C, \quad (8)$$

where \circ denotes $A \circ B = \int d\tau'' A(\tau, \tau'') B(\tau'', \tau')$ and the self-energy is given by $\Sigma_{11\sigma}^C(\tau, \tau') = i\zeta g_\eta^C(\tau, \tau') G_{11\bar{\sigma}}^C(\tau', \tau)$. By using the statistical properties of the noise fields, the retarded, advanced and Keldysh components of the self-energy take the form: $\Sigma_\sigma^{R/A/K}(\tau, \tau') = i\zeta g_\eta^{R/A/K}(\tau, \tau') n_{0\bar{\sigma}}$. Here, $n_{0\bar{\sigma}}$ denotes the average occupation number of the opposite spin $\bar{\sigma}$ at the quantum dot, satisfying the following self-consistent integral equation [46]:

$$n_{0\sigma} = \int \frac{d\omega}{2\pi} \frac{\Gamma_\sigma(\omega) [n_{L\sigma}(\omega) + n_{R\sigma}(\omega)]}{[\omega - \epsilon_0 - R_\sigma(\omega)]^2 + [\Gamma_\sigma(\omega) + \frac{\gamma}{2} n_{0\bar{\sigma}}]^2}, \quad (9)$$

where $n_{L(R)\sigma}(\omega) = [e^{(\omega - \Delta\mu_{L(R)\sigma})/T_{L(R)}} - \zeta]^{-1}$ is the Fermi or Bose distribution function of the left (right) reservoir. The chemical potential difference from the origin of the frequencies is defined as $\Delta\mu_{L(R)\sigma} = \mu_{L(R)\sigma} - \sum_{s\sigma'} \mu_{s\sigma'}/4$ and $T_{L(R)}$ denotes the reservoir temperature. The quantities $R_\sigma(\omega) = 2 \sum_{\mathbf{k}} |t_{\mathbf{k}}|^2 \text{Re}[g_{s\sigma}^R(\mathbf{k}, \omega)]$ and $\Gamma_\sigma(\omega) = -2 \sum_{\mathbf{k}} |t_{\mathbf{k}}|^2 \text{Im}[g_{s\sigma}^R(\mathbf{k}, \omega)]$ represent the energy shifts induced by the reservoir. By using $\text{Im}[g_{s\sigma}^R] \propto \delta(\omega + \mu - \epsilon_{\mathbf{k}})$ with $\mu = \sum_{s\sigma} \mu_{s\sigma}/4$, the particle and energy currents are given by [46]

$$I = \sum_\sigma \int \frac{d\omega}{2\pi} \left[\mathcal{T}_\sigma(\omega) + \frac{\mathcal{L}_\sigma(\omega)}{2} \right] [n_{L\sigma}(\omega) - n_{R\sigma}(\omega)], \quad (10)$$

$$I_E = \sum_\sigma \int \frac{d\omega}{2\pi} (\omega + \mu) \left[\mathcal{T}_\sigma(\omega) + \frac{\mathcal{L}_\sigma(\omega)}{2} \right] \times [n_{L\sigma}(\omega) - n_{R\sigma}(\omega)], \quad (11)$$

where $\mathcal{T}_\sigma(\omega)$ and $\mathcal{L}_\sigma(\omega)$ respectively represent the transmittance and loss probability defined as

$$\mathcal{T}_\sigma(\omega) = \frac{[\Gamma_\sigma(\omega)]^2}{[\omega - \epsilon_0 - R_\sigma(\omega)]^2 + [\Gamma_\sigma(\omega) + \frac{\gamma}{2} n_{0\bar{\sigma}}]^2}, \quad (12)$$

$$\mathcal{L}_\sigma(\omega) = \frac{\Gamma_\sigma(\omega) \gamma n_{0\bar{\sigma}}}{[\omega - \epsilon_0 - R_\sigma(\omega)]^2 + [\Gamma_\sigma(\omega) + \frac{\gamma}{2} n_{0\bar{\sigma}}]^2}. \quad (13)$$

We compare the above results with those for the one-body loss case [34]. A key similarity is that the formal expressions for the particle and energy currents remain identical for bosons and fermions in both cases. However, a crucial difference lies in the structure of the effective dissipation: in the two-body loss case, the effective loss strength is given by $\gamma n_{0\bar{\sigma}}$ [49]. This occupation-dependent term leads to differences in the particle and

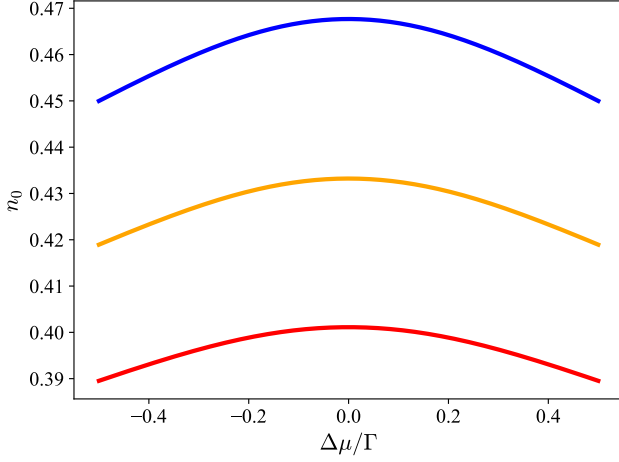


FIG. 3. The average number of particle at the central dot with two-body loss. The temperature is set to $T/\Gamma = 0.1$. The blue, orange and red curves correspond to $\gamma/\Gamma = 0.1, 0.5$ and 1.0, respectively.

energy currents between one-body and two-body loss cases.

For the sake of an analytic comparison between one-body and two-body loss effects, we now consider the case of two-component fermions at zero temperature. Especially, we focus on particle transport near the Fermi level, assuming $R_\sigma(\omega) \rightarrow 0$ and $\Gamma_\sigma(\omega) \rightarrow \Gamma$ with $\epsilon = 0$, $\mu_{L(R)\sigma} = \mu_{L(R)}$ and $\Delta\mu = \mu_L - \mu_R \ll \frac{\mu_L + \mu_R}{2}$ [50]. Under these assumptions, spin-up and spin-down particles are equally populated $n_{0\uparrow} = n_{0\downarrow} = n_0 = (\sqrt{1 + \gamma/\Gamma} - 1)/(\gamma/\Gamma)$, and the particle current follows an Ohmic relation $I = G\Delta\mu$ with conductance G . The resulting expressions for the conductance are

$$G_1 = \frac{2}{2\pi} \cdot \frac{1}{1 + \gamma/2\Gamma}, \quad G_2 = \frac{2}{2\pi} \cdot \frac{2}{1 + \sqrt{1 + \gamma/\Gamma}}, \quad (14)$$

where G_1 and G_2 correspond to the conductance in the one-body and two-body loss cases, respectively. Here, $1/2\pi$ is the conductance quantum in natural units and the prefactor 2 accounts for spin degeneracy [51]. These expressions demonstrate that $G_2 > G_1$, i.e., the particle current is more strongly suppressed by one-body loss than two-body loss. This finding agrees with the recent experimental observation [26].

We emphasize that these essential results persist under a finite bias at nonzero temperature $T_{L(R)} = T > 0$, whose numerical results are shown in Fig. 3. As in the zero-temperature case, n_0 decreases with increasing γ . Notably, at finite temperature, n_0 also decreases with increasing $|\Delta\mu|$, a feature absent at zero temperature.

Figure 4 compares particle currents under one-body and two-body losses. For $\gamma/\Gamma \in [0.1, 1]$, the occupation $n_0 < 1$ (Fig. 3), and the denominator of $\mathcal{T}_\sigma(\omega) + \mathcal{L}_\sigma(\omega)/2$ decreases more rapidly than the numerator. Consequently, the particle current in the presence of two-body

loss exceeds that in one-body loss. This indicates that the inequality $G_2 > G_1$ remains robust even under thermal fluctuations.

We can also discuss effects of an interaction in the channel. For fermions, the Hamiltonian of the system is reduced to the Anderson model [48], where $H_{1D}^0 \rightarrow \sum_\sigma \epsilon_0 d_{0\sigma}^\dagger d_{0\sigma} + U d_{0\uparrow}^\dagger d_{0\uparrow} d_{0\downarrow}^\dagger d_{0\downarrow}$. In the two-terminal experiments with normal reservoirs in ultracold atomic gases, the interaction is weak such that the renormalization effect associated with the Kondo effect is negligible [27]. In such a regime, the following mean-field approximation is allowed [52]: $H_{1D}^0 \approx \sum_\sigma (\epsilon_0 + U n_{0\bar{\sigma}}) d_{0\sigma}^\dagger d_{0\sigma}$. The resultant expressions of the particle and energy currents correspond to ones by considering the energy-shift $\epsilon_0 \rightarrow \epsilon_0 + U n_{0\bar{\sigma}}$.

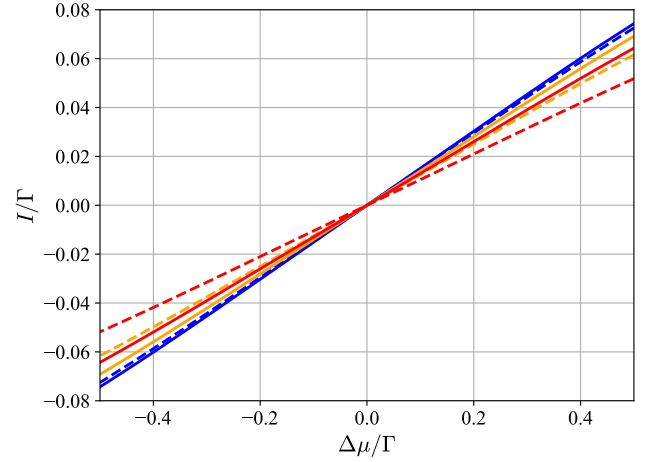


FIG. 4. Comparison between one- and two-body loss effects on the particle current. The temperature is set to $T/\Gamma = 0.1$. The blue, orange and red curves correspond to $\gamma/\Gamma = 0.1, 0.5$ and 1.0, respectively. The solid ones represent results with two-body loss, while the dashed ones indicate those with one-body loss.

Multi-site case.—We now turn to the multi-site case. Under the symmetry of the system $\epsilon_{-i} = \epsilon_i$ and $t_{-i} = t_i$ for $i = 1, 2, \dots, N$, Green's function obeys the following relation: $G_{ij\sigma}^R(\omega) = G_{ji\sigma}^R(\omega) = G_{(M-j+1)(M-i+1)\sigma}^R(\omega)$. By using above, we obtain [46]

$$I = \sum_\sigma \int \frac{d\omega}{2\pi} \left[\mathcal{T}_\sigma^M(\omega) + \frac{\mathcal{L}_\sigma^M(\omega)}{2} \right] [n_{L\sigma}(\omega) - n_{R\sigma}(\omega)], \quad (15)$$

$$I_E = \sum_\sigma \int \frac{d\omega}{2\pi} (\omega + \mu) \left[\mathcal{T}_\sigma^M(\omega) + \frac{\mathcal{L}_\sigma^M(\omega)}{2} \right] \times [n_{L\sigma}(\omega) - n_{R\sigma}(\omega)], \quad (16)$$

where

$$\mathcal{T}_\sigma^M(\omega) = \left[\Gamma_\sigma(\omega) \right]^2 \left| G_{1M\sigma}^R(\omega) \right|^2, \quad (17)$$

$$\mathcal{L}_\sigma^M(\omega) = \left[\Gamma_\sigma(\omega) \gamma n_{0\bar{\sigma}} \right] \left| G_{1\frac{M+1}{2}\sigma}^R(\omega) \right|^2. \quad (18)$$

These expressions are analogous to the single-site case ($M = 1$).

Finally, we point out the particle-loss rate, which can also be evaluated with the Keldysh formalism as follows [46]:

$$-\dot{N} = - \sum_\sigma \left[\dot{N}_{L\sigma} + \dot{N}_{R\sigma} \right] = 2\gamma n_{0\uparrow} n_{0\downarrow}. \quad (19)$$

This result is intuitively reasonable, since the particle loss rate increases with both the number of spin-up and spin-down particles at the lossy site and the strength of the dissipation. We note that Eq. (19) remains valid regardless of the total number of sites.

Conclusion.—We have theoretically investigated quantum transport through the 1D chain subject to localized two-body loss. For fermions, in contrast to the one-body loss case, the dissipation strength in our model acquires

an occupation-dependent character, leading to a weaker suppression of the particle current in the weakly dissipative regime. This mechanism may provide a natural explanation for a recent observation in a superfluid junction [26]. For direct quantitative comparison, similar experiments using normal (non-superfluid) reservoirs would be highly desirable. Such setups are feasible in ultracold atomic systems by tuning interactions via Feshbach resonances. Finally, it would be theoretically compelling to extend the present field-theory framework to the strongly dissipative regime, where a dissipation-induced Kondo effect has been predicted for the single-site case [49, 53, 54]. Extending it to multi-site systems and elucidating crossover from weak to strong dissipation within a field-theoretic analysis remain an important direction for future work.

ACKNOWLEDGMENT

We are also grateful to T. Esslinger, P. Fabritius, T. Giamarchi, M.-Z. Huang, J. Mohan, M. Talebi, A.-M. Visuri, and S. Wili for discussions. This work is supported by JST PRESTO (JPMJPR235) and JSPS KAKENHI (JP25K07191).

-
- [1] H.-P. Breuer and F. Petruccione, *The theory of open quantum systems* (OUP Oxford, 2002).
 - [2] H. M. Wiseman and G. J. Milburn, *Quantum measurement and control* (Cambridge university press, 2009).
 - [3] Y. V. Nazarov and Y. M. Blanter, *Quantum transport: introduction to nanoscience* (Cambridge university press, 2009).
 - [4] E. G. D. Torre, E. Demler, T. Giamarchi, and E. Altman, Quantum critical states and phase transitions in the presence of non-equilibrium noise, *Nat. Phys.* **6**, 806 (2010).
 - [5] E. G. D. Torre, E. Demler, T. Giamarchi, and E. Altman, Dynamics and universality in noise-driven dissipative systems, *Phys. Rev. B* **85**, 184302 (2012).
 - [6] B. Misra and E. C. G. Sudarshan, The zeno's paradox in quantum theory, *J. Math. Phys.* **18**, 756 (1977).
 - [7] M. C. Fischer, B. Gutiérrez-Medina, and M. G. Raizen, Observation of the quantum zeno and anti-zeno effects in an unstable system, *Phys. Rev. Lett.* **87**, 040402 (2001).
 - [8] P. Facchi and S. Pascazio, Quantum zeno subspaces, *Phys. Rev. Lett.* **89**, 080401 (2002).
 - [9] N. Syassen, D. M. Bauer, M. Lettner, T. Volz, D. Dietze, J. J. García-Ripoll, J. I. Cirac, G. Rempe, and S. Dür, Strong dissipation inhibits losses and induces correlations in cold molecular gases, *Science* **320**, 1329 (2008).
 - [10] P. Facchi and S. Pascazio, Quantum zeno dynamics: mathematical and physical aspects, *J. Phys. A: Math. Theor.* **41**, 493001 (2008).
 - [11] Y. Sun, T. Shi, Z. Liu, Z. Zhang, L. Xiao, S. Jia, and Y. Hu, Fractional quantum zeno effect emerging from non-hermitian physics, *Phys. Rev. X* **13**, 031009 (2023).
 - [12] Y. Ashida, S. Furukawa, and M. Ueda, Parity-time-symmetric quantum critical phenomena, *Nature communications* **8**, 15791 (2017).
 - [13] M. Nakagawa, N. Kawakami, and M. Ueda, Non-hermitian kondo effect in ultracold alkaline-earth atoms, *Phys. Rev. Lett.* **121**, 203001 (2018).
 - [14] A. J. Daley, Quantum trajectories and open many-body quantum systems, *Adv. Phys.* **63**, 77 (2014).
 - [15] M. Müller, S. Diehl, G. Pupillo, and P. Zoller, Engineered open systems and quantum simulations with atoms and ions, *Adv. At. Mol. Opt. Phys.* **61**, 1–80 (2012).
 - [16] L. M. Sieberer, M. Buchhold, and S. Diehl, Keldysh field theory for driven open quantum systems, *Rep. Prog. Phys.* **79**, 096001 (2016).
 - [17] G. Barontini, R. Labouvie, F. Stubenrauch, A. Vogler, V. Guarrera, and H. Ott, Controlling the dynamics of an open many-body quantum system with localized dissipation, *Phys. Rev. Lett.* **110**, 035302 (2013).
 - [18] R. Labouvie, B. Santra, S. Heun, S. Wimberger, and H. Ott, Negative differential conductivity in an interacting quantum gas, *Phys. Rev. Lett.* **115**, 050601 (2015).
 - [19] R. Labouvie, B. Santra, S. Heun, and H. Ott, Bistability in a driven-dissipative superfluid, *Phys. Rev. Lett.* **116**, 235302 (2016).
 - [20] Y. S. Patil, S. Chakram, and M. Vengalattore, Measurement-induced localization of an ultracold lattice gas, *Phys. Rev. Lett.* **115**, 140402 (2015).
 - [21] H. P. Lüschen, P. Bordia, S. S. Hodgman, M. Schreiber, S. Sarkar, A. J. Daley, M. H. Fischer, E. Altman, I. Bloch, and U. Schneider, Signatures of many-body localization in a controlled open quantum system, *Phys. Rev. X* **7**, 011034 (2017).

- [22] M. J. Mark, E. Haller, K. Lauber, J. G. Danzl, A. Janisch, H. P. Büchler, A. J. Daley, and H.-C. Nägerl, Preparation and spectroscopy of a metastable mott-insulator state with attractive interactions, *Phys. Rev. Lett.* **108**, 215302 (2012).
- [23] B. Yan, S. A. Moses, B. Gadway, J. P. C. K. R. Hazzard, A. M. Rey, D. S. Jin, and J. Ye, Observation of dipolar spin-exchange interactions with lattice-confined polar molecules, *Nature* **501**, 521 (2013).
- [24] T. Tomita, S. Nakajima, I. Danshita, Y. Takasu, and Y. Takahashi, Observation of the mott insulator to superfluid crossover of a driven-dissipative bose-hubbard system, *Sci. Adv.* **3**, e1701513 (2017).
- [25] T. Tomita, S. Nakajima, Y. Takasu, and Y. Takahashi, Dissipative bose-hubbard system with intrinsic two-body loss, *Phys. Rev. A* **99**, 031601(R) (2019).
- [26] M.-Z. Huang, P. Fabritius, J. Mohan, M. Talebi, S. Wili, and T. Esslinger, Limited thermal and spin transport in a dissipative superfluid junction (2024), arXiv:2412.08525v1 [cond-mat.quant-gas].
- [27] S. Krinner, T. Esslinger, and J.-P. Brantut, Two-terminal transport measurements with cold atoms, *Journal of Physics: Condensed Matter* **29**, 343003 (2017).
- [28] L. Amico, D. Anderson, M. Boshier, J.-P. Brantut, L.-C. Kwek, A. Minguzzi, and W. von Klitzing, Colloquium: Atomtronic circuits: From many-body physics to quantum technologies, *Rev. Mod. Phys.* **94**, 041001 (2022).
- [29] L. Corman, P. Fabritius, S. Häusler, J. Mohan, L. H. Dogra, D. Husmann, M. Lebrat, and T. Esslinger, Quantized conductance through a dissipative atomic point contact, *Phys. Rev. A* **100**, 053605 (2019).
- [30] H. Fröml, C. Muckel, C. Kollath, A. Chiocchetta, and S. Diehl, Ultracold quantum wires with localized losses: Many-body quantum zeno effect, *Phys. Rev. B* **101**, 144301 (2020).
- [31] H. Fröml, A. Chiocchetta, C. Kollath, and S. Diehl, Fluctuation-induced quantum zeno effect, *Phys. Rev. Lett.* **122**, 040402 (2019).
- [32] M. Lebrat, S. Häusler, P. Fabritius, D. Husmann, L. Corman, and T. Esslinger, Quantized conductance through a spin-selective atomic point contact, *Phys. Rev. Lett.* **123**, 193605 (2019).
- [33] A.-M. Visuri, T. Giamarchi, and C. Kollath, Symmetry-protected transport through a lattice with a local particle loss, *Phys. Rev. Lett.* **129**, 056802 (2022).
- [34] S. Uchino, Comparative study for two-terminal transport through a lossy one-dimensional quantum wire, *Phys. Rev. A* **106**, 053320 (2022).
- [35] M.-Z. Huang, J. Mohan, A.-M. Visuri, P. Fabritius, M. Talebi, S. Wili, S. Uchino, T. Giamarchi, and T. Esslinger, Superfluid signatures in a dissipative quantum point contact, *Phys. Rev. Lett.* **130**, 200404 (2023).
- [36] A.-M. Visuri, J. Mohan, S. Uchino, M.-Z. Huang, T. Esslinger, and T. Giamarchi, Dc transport in a dissipative superconducting quantum point contact, *Phys. Rev. Res.* **5**, 033095 (2023).
- [37] M. Gievers, T. Müller, H. Fröml, S. Diehl, and A. Chiocchetta, Quantum wires with local particle loss: Transport manifestations of fluctuation-induced effects, *Phys. Rev. B* **110**, 205419 (2024).
- [38] A. Kamenev, *Field theory of non-equilibrium systems* (Cambridge University Press, 2023).
- [39] S. Datta, *Electronic transport in mesoscopic systems* (Cambridge university press, 1997).
- [40] C. W. Gardiner and P. Zoller, *Quantum Noise*, 3rd ed. (Springer, Berlin, 2004).
- [41] P. E. Dolgirev, J. Marino, D. Sels, and E. Demler, Non-gaussian correlations imprinted by local dephasing in fermionic wires, *Phys. Rev. B* **102**, 100301(R) (2020).
- [42] T. Jin, J. a. S. Ferreira, M. Filippone, and T. Giamarchi, Exact description of quantum stochastic models as quantum resistors, *Phys. Rev. Res.* **4**, 013109 (2022).
- [43] A. Altland and B. Simons, *Condensed Matter Field Theory*, 3rd ed. (Cambridge university press, Cambridge, 2023).
- [44] L. Pan, X. Chen, Y. Chen, and H. Zhai, Non-hermitian linear response theory, *Nat. Phys.* **16**, 767 (2020).
- [45] X.-X. Yang, B.-H. Wu, Y. Chen, and W. Zhang, *f*-sum rules for dissipative systems, *Phys. Rev. Lett.* **133**, 100401 (2024).
- [46] See Supplemental Material for theoretical analyses in details.
- [47] H. Haug and A.-P. Jauho, *Quantum Kinetics in Transport and Optics of Semiconductors* (Springer, Berlin, 2008).
- [48] H. Bruus and K. Flensberg, *Many-body quantum theory in condensed matter physics: an introduction* (Oxford university press, 2004).
- [49] Y.-F. Qu, M. Stefanini, T. Shi, T. Esslinger, S. Gopalakrishnan, J. Marino, and E. Demler, Variational approach to the dynamics of dissipative quantum impurity models, *Phys. Rev. B* **111**, 155113 (2025).
- [50] Notice that $\epsilon = 0$ represents that the channel transmittance at the Fermi level is 1 in the absence of dissipation.
- [51] Here, the conductance in neutral systems is given. In the case of electric systems, the conductance quantum becomes $e^2/2\pi$ in natural units.
- [52] K. Yamada, Perturbation expansion for the anderson hamiltonian. ii, *Progress of Theoretical Physics* **53**, 970 (1975).
- [53] M. Stefanini, Y.-F. Qu, T. Esslinger, S. Gopalakrishnan, E. Demler, and J. Marino, Dissipative realization of kondo models, *Communications Physics* **8**, 212 (2025).
- [54] M. Sonner, V. Link, and D. A. Abanin, Semi-group influence matrices for non-equilibrium quantum impurity models, arXiv preprint arXiv:2502.00109 (2025).